Anomalous transport effects from the Berry curvature point of view: symmetries and different mechanisms

Jonathan Noky

July 8th, 2022

MAX PLANCK INSTITUTE FOR CHEMICAL PHYSICS OF SOLIDS

NÖTHNITZER STR. 40
01187 DRESDEN, GERMANY

Anomalous transport in topological metals

Cubic Heusler compounds

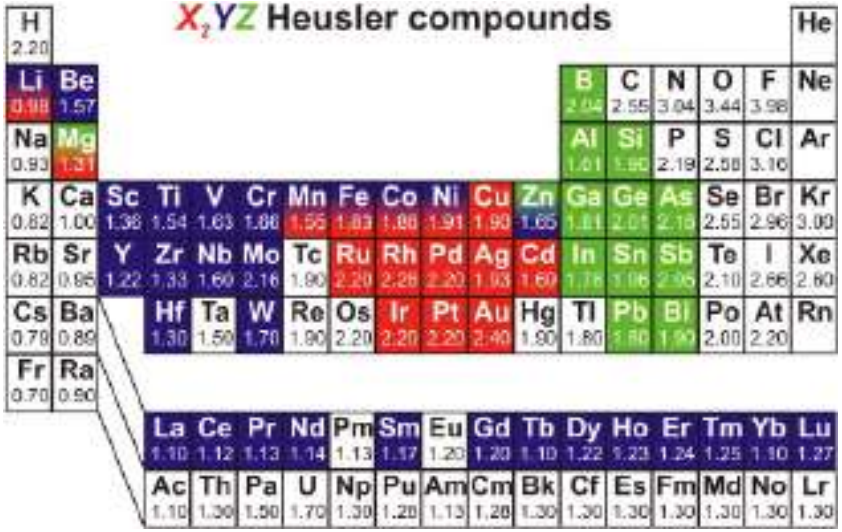

[1] T. Graf *et al.*, Progress in Solid State Chemistry **39**, 1 (2011)

Anomalous transport in topological metals

Cubic Heusler compounds

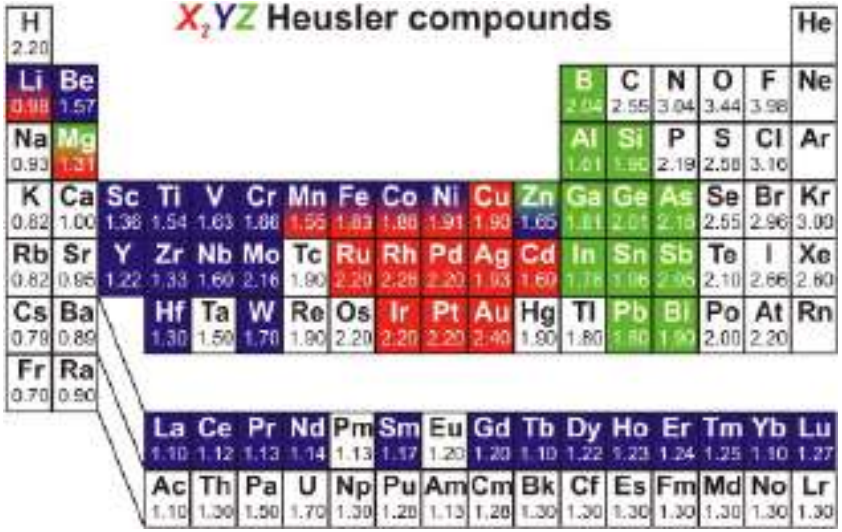

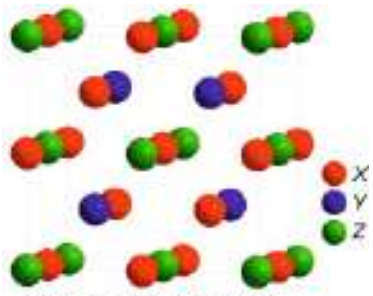

Inverse (SG 216)

X -X -Y -Z

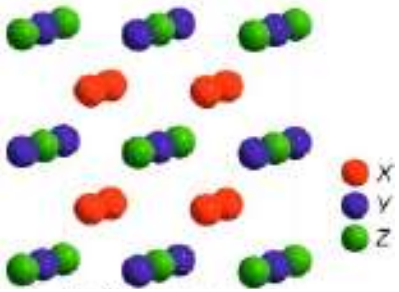

Regular (SG 225)

X -Y -X -Z

- Four interpenetrating *fcc* lattices

[1] T. Graf *et al.*, Progress in Solid State Chemistry **39**, 1 (2011)

Anomalous transport in topological metals

Cubic Heusler compounds

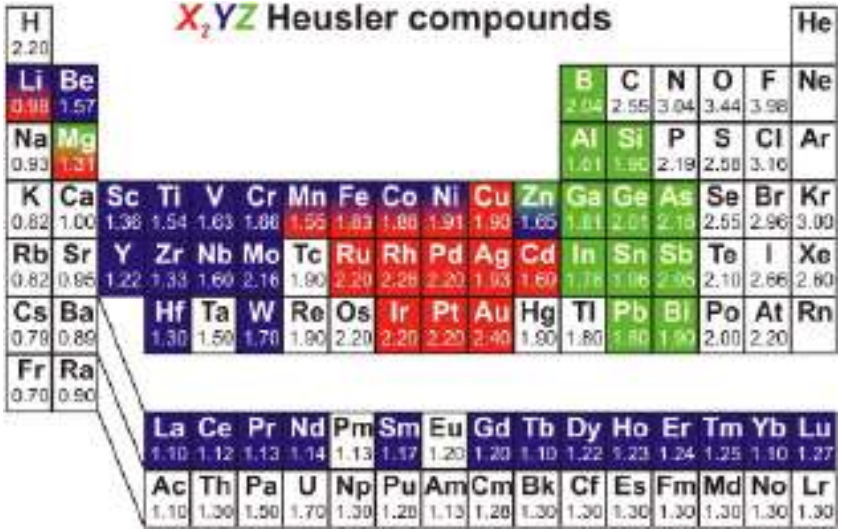

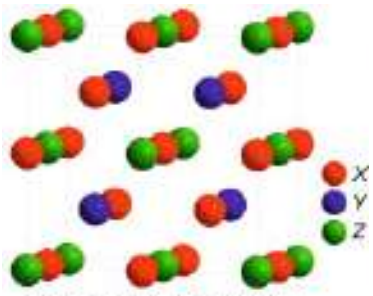

Inverse (SG 216)

X -X -Y -Z

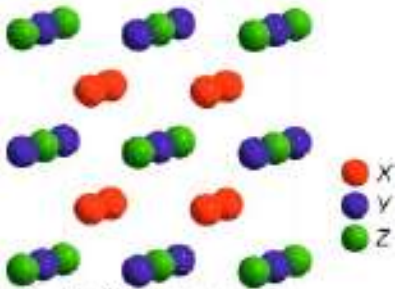

Regular (SG 225)

X -Y -X -Z

- Four interpenetrating *fcc* lattices
- Host both magnetism and topological band structures
- Large AHE and ANE possible, e. g. in Co_2MnGa[2]

→ promising class of materials to study anomalous transport

[1] T. Graf *et al.*, Progress in Solid State Chemistry **39**, 1 (2011)

[2] S. Guin, ..., JN *et al.*, NPG Asia Materials **11**, 16 (2019)

Anomalous transport in topological metals

Anomalous Hall and Nernst effects

Anomalous Hall effect

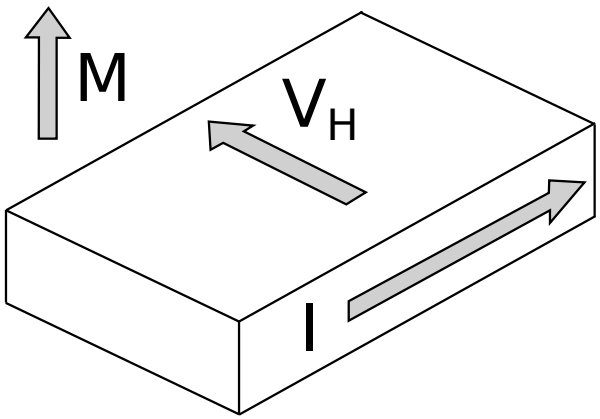

$$\vec{j} = \underline{\sigma}\vec{E}$$

Intrinsic deflection

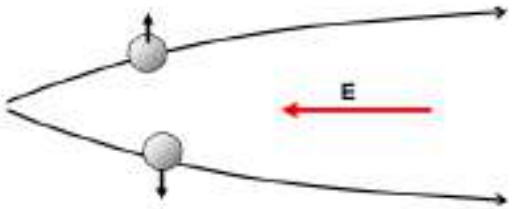

Side jump

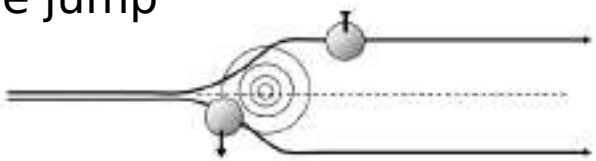

Skew scattering

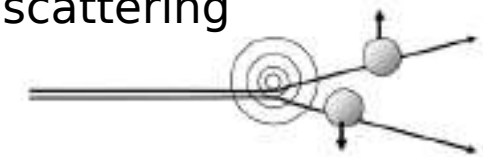

[3] N. Nagaosa *et al.*, Review of Modern Physics **82**, 1539 (2010)

Anomalous transport in topological metals

Anomalous Hall and Nernst effects

Anomalous Hall effect

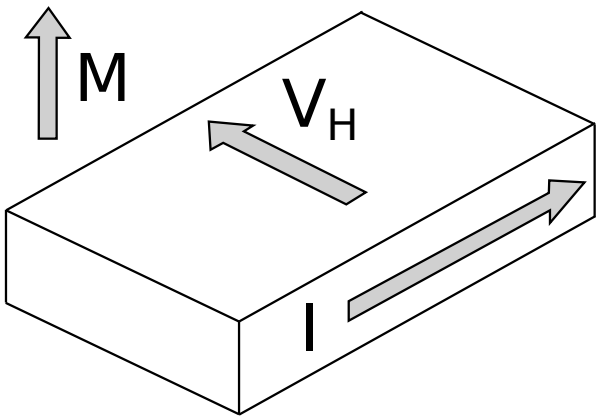

$$\vec{j} = \underline{\underline{\sigma}}\vec{E}$$

Intrinsic deflection

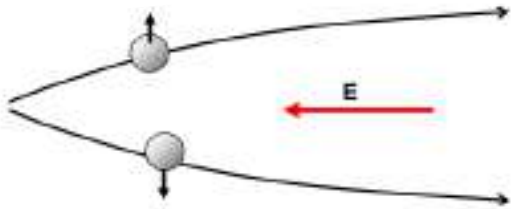

Side jump

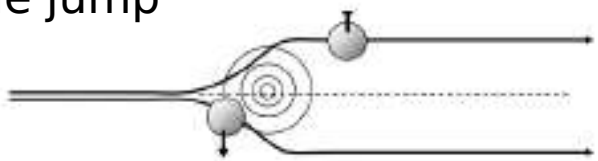

Skew scattering

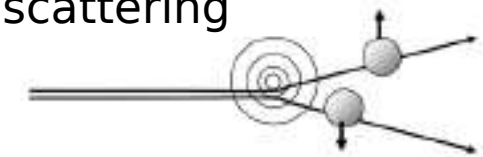

Intrinsic contribution

$$\sigma_{ij} = \frac{e^2}{\hbar}\sum_n \int \frac{d^3k}{(2\pi)^3}\Omega_{ij}^{n\mathbf{k}} f_{n\mathbf{k}}$$

[3] N. Nagaosa *et al.*, Review of Modern Physics **82**, 1539 (2010)

Anomalous transport in topological metals

Anomalous Hall and Nernst effects

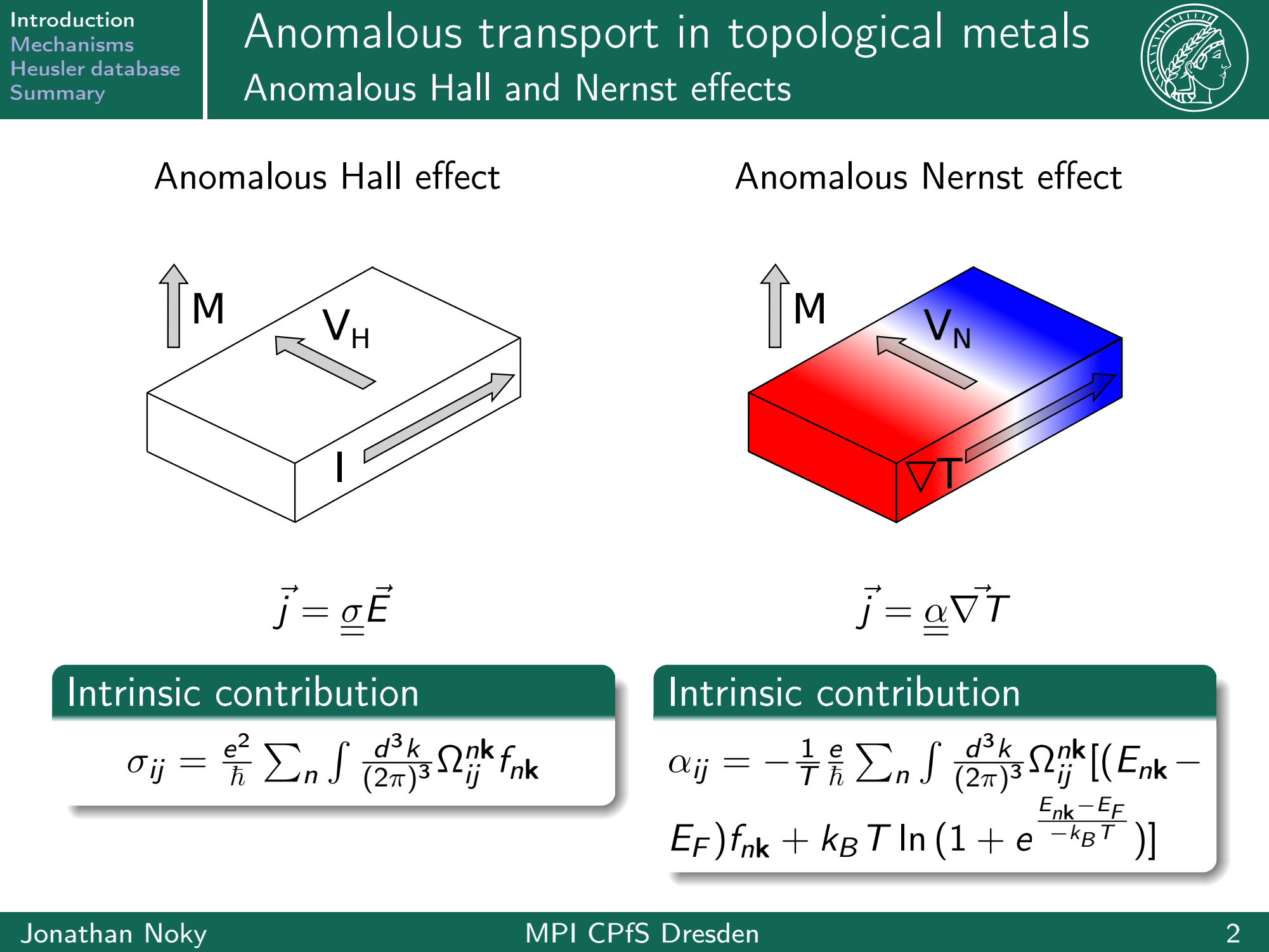

Anomalous Hall effect

$$\vec{j} = \underline{\underline{\sigma}}\vec{E}$$

Intrinsic contribution

$$\sigma_{ij} = \frac{e^2}{\hbar}\sum_n \int \frac{d^3k}{(2\pi)^3}\Omega_{ij}^{n\mathbf{k}} f_{n\mathbf{k}}$$

Anomalous Nernst effect

$$\vec{j} = \underline{\underline{\alpha}}\vec{\nabla T}$$

Intrinsic contribution

$$\alpha_{ij} = -\frac{1}{T}\frac{e}{\hbar}\sum_n \int \frac{d^3k}{(2\pi)^3}\Omega_{ij}^{n\mathbf{k}}[(E_{n\mathbf{k}} - E_F)f_{n\mathbf{k}} + k_B T \ln\left(1 + e^{\frac{E_{n\mathbf{k}}-E_F}{-k_B T}}\right)]$$

Anomalous transport in topological metals
AHE with M=0

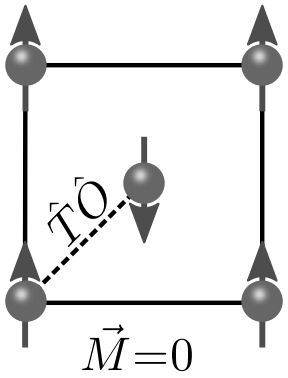

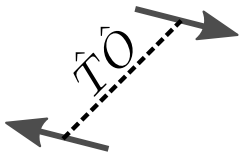

$\vec{\Omega}(\vec{k})=-\vec{\Omega}(\hat{T}\hat{O}\vec{k})$

$\vec{\sigma}=\int dk\vec{\Omega}=0$

- Goal: search for anomalous Hall effect (AHE) without net magnetic moment
- Possible in non-collinear AFMs like Mn_3Ge
- In collinear AFMs with symmetry $\hat{T}\hat{O}$ no AHE allowed

[4] A. K. Nayak et al., *Sci. Adv.* 2: e1501870 (2016)

Anomalous transport in topological metals
AHE with M=0

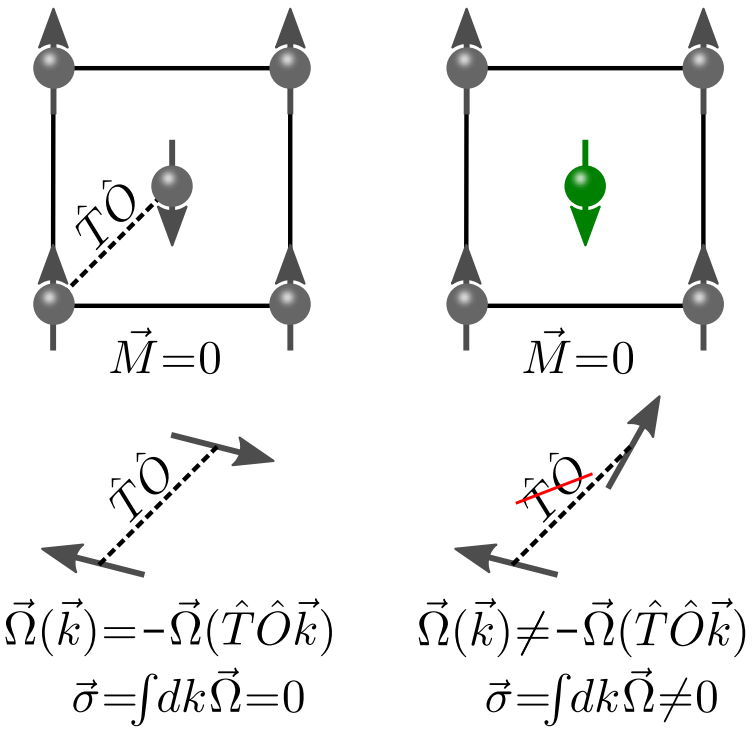

- Goal: search for anomalous Hall effect (AHE) without net magnetic moment
- Possible in non-collinear AFMs like Mn_3Ge
- In collinear AFMs with symmetry $\hat{T}\hat{O}$ no AHE allowed
- Change type of one atom in the AFM $\rightarrow$ $\hat{T}\hat{O}$ broken $\rightarrow$ AHE possible

[4] A. K. Nayak et al., *Sci. Adv.* 2: e1501870 (2016)

Anomalous transport in topological metals

Model for a ferrimagnetic Weyl system

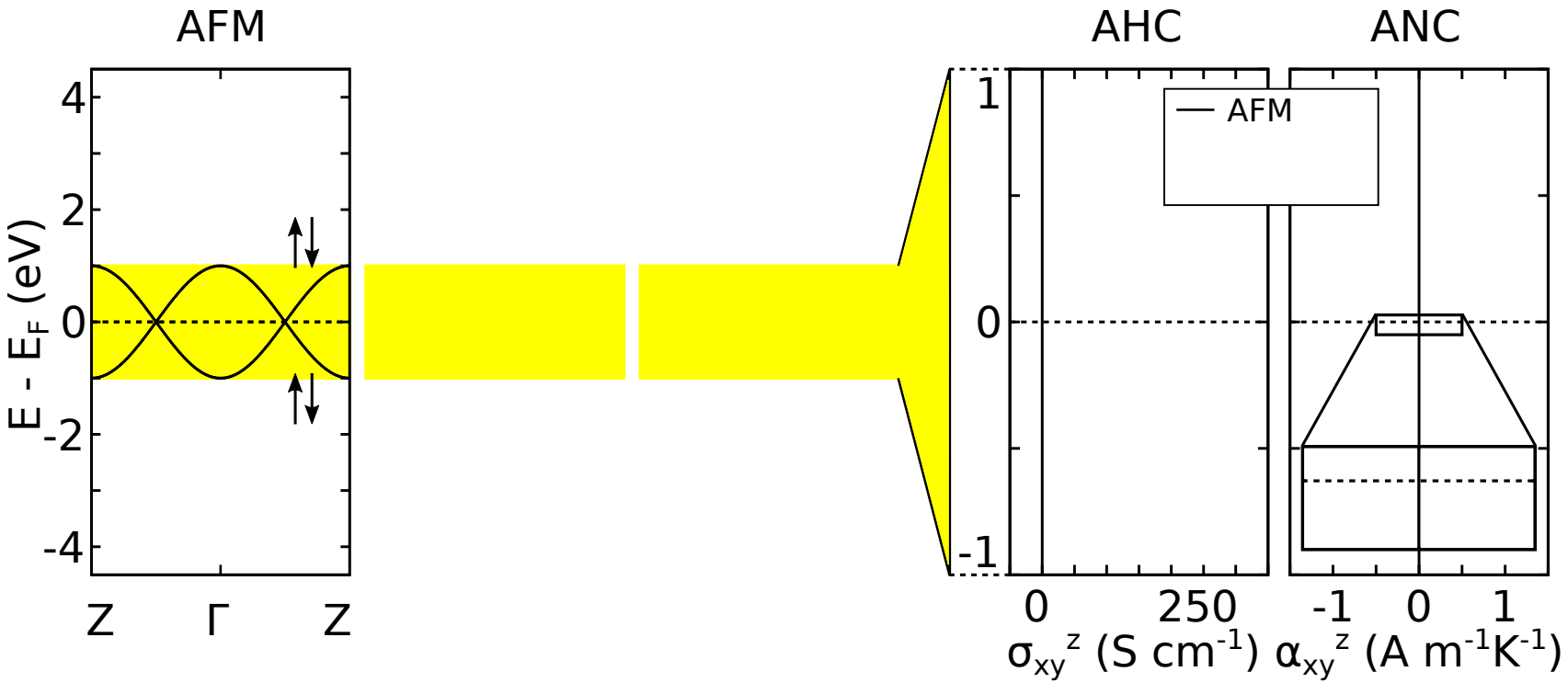

- Model from Lu *et al.*[5]: AFM with Dirac like crossings at E_F

[5] H.-Z. Lu *et al.*, Physical Review B **92**, 045203 (2015)

Anomalous transport in topological metals

Model for a ferrimagnetic Weyl system

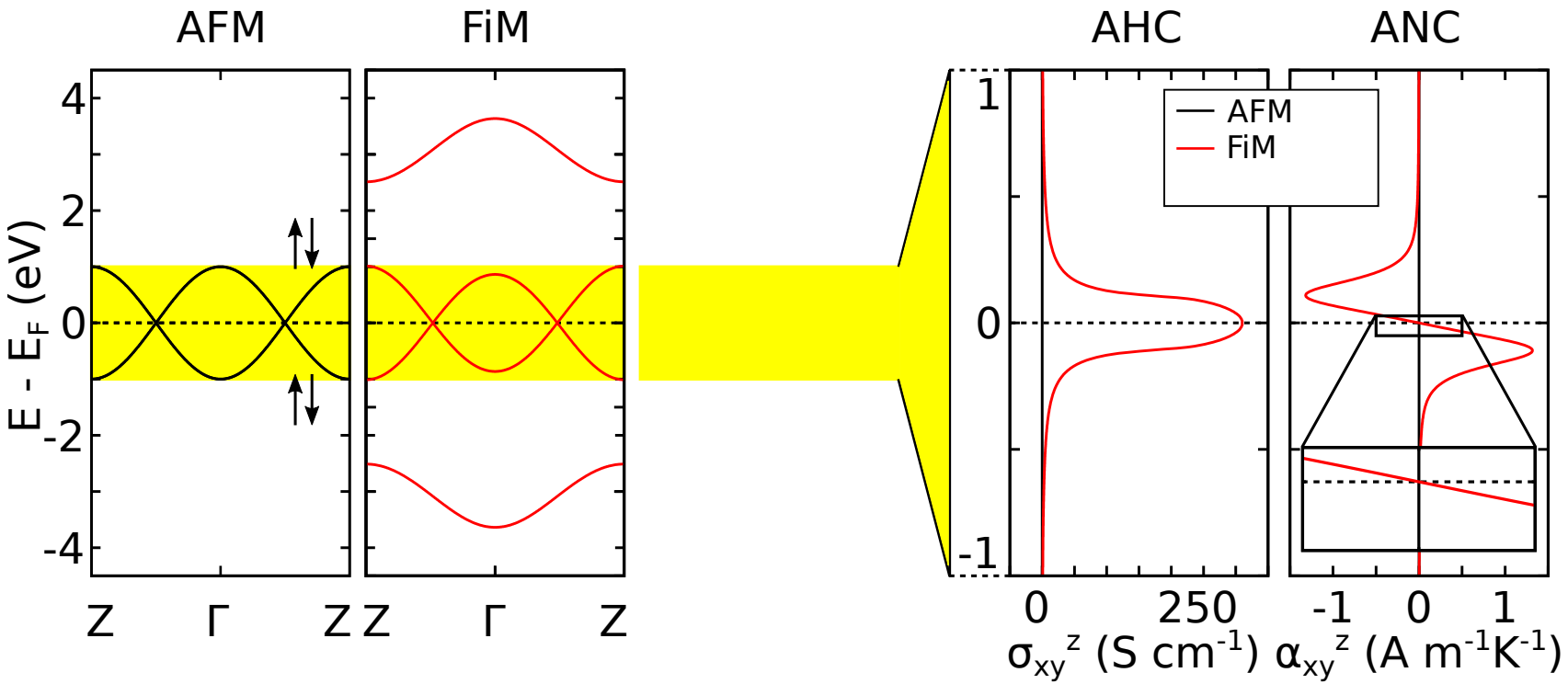

- Model from Lu *et al.*[5]: AFM with Dirac like crossings at E_F
- Ferrimagnet with Weyl crossings $\rightarrow$ strong BC

[5] H.-Z. Lu *et al.*, Physical Review B **92**, 045203 (2015)

Anomalous transport in topological metals

Model for a ferrimagnetic Weyl system

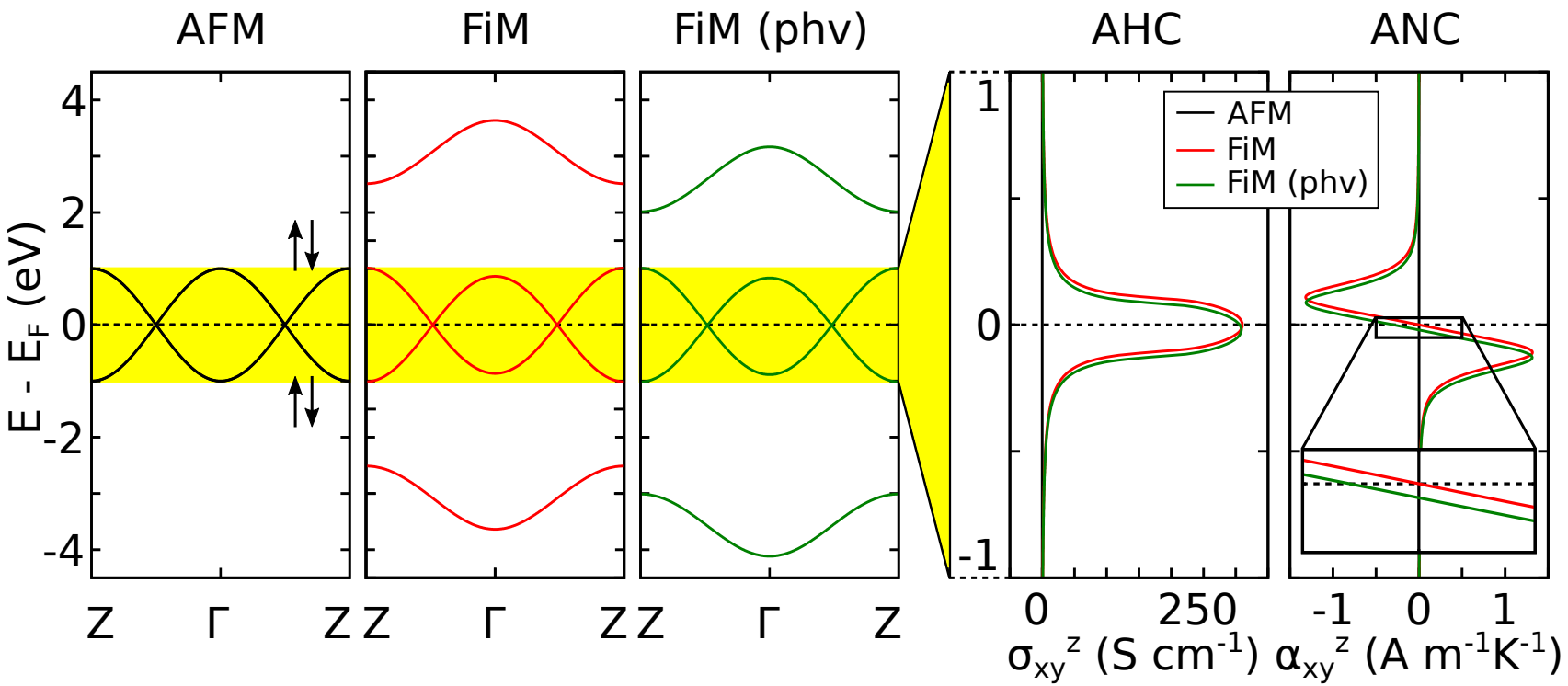

- Model from Lu *et al.*[5]: AFM with Dirac like crossings at E_F
- Ferrimagnet with Weyl crossings $\rightarrow$ strong BC
- Asymmetric Ferrimagnet $\rightarrow$ non-zero ANC[5]

[5] H.-Z. Lu *et al.*, Physical Review B **92**, 045203 (2015)
[6] JN *et al.*, Physical Review B 97, 220405(R) (2018)

Anomalous transport in topological metals

Ti_2MnAl - Weyl points at the Fermi level

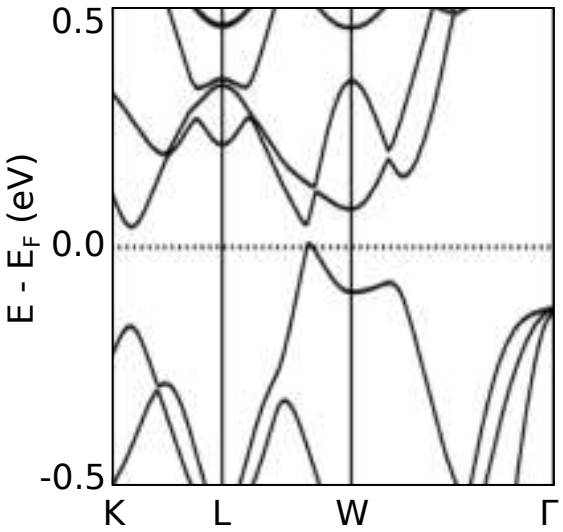

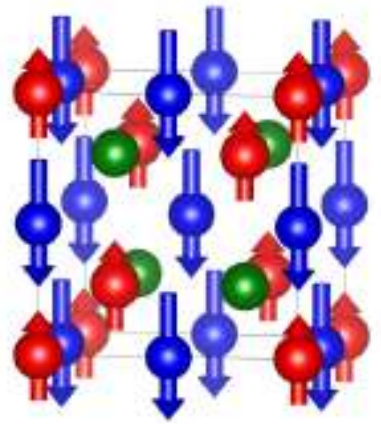

- Ferrimagnet with vanishing net magnetic moment
- Clean Fermi surface with Weyl points slightly above

[6] JN *et al.*, Physical Review B 97, 220405(R) (2018)

Anomalous transport in topological metals

Ti_2MnAl - Weyl points at the Fermi level

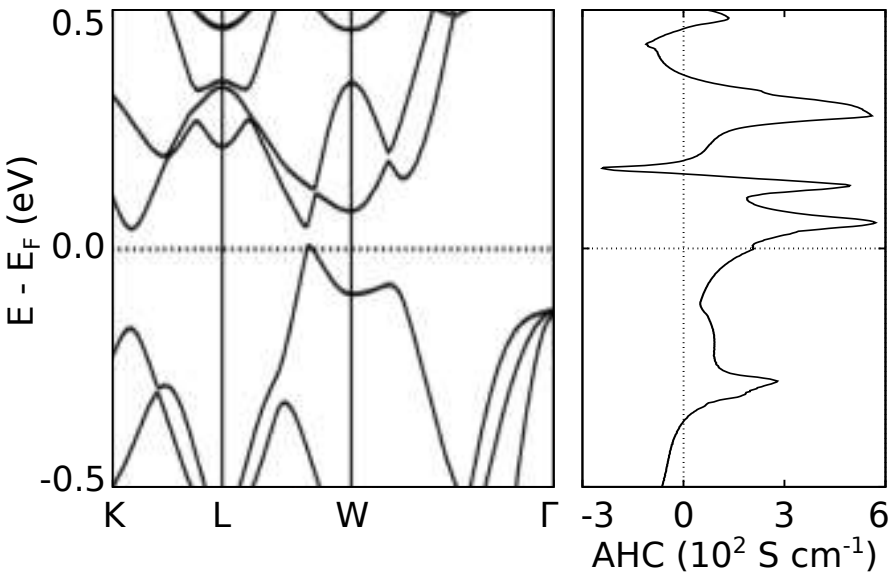

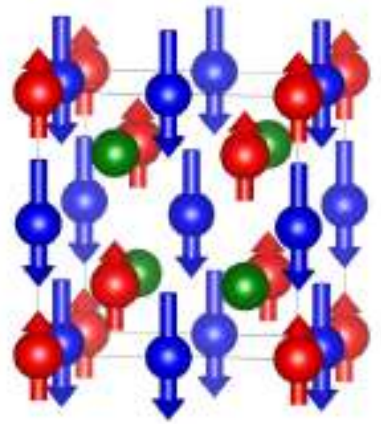

- Ferrimagnet with vanishing net magnetic moment
- Clean Fermi surface with Weyl points slightly above
- Peak in the AHC at Weyl point energy

[6] JN *et al.*, Physical Review B 97, 220405(R) (2018)

Anomalous transport in topological metals

Ti_2MnAl - Weyl points at the Fermi level

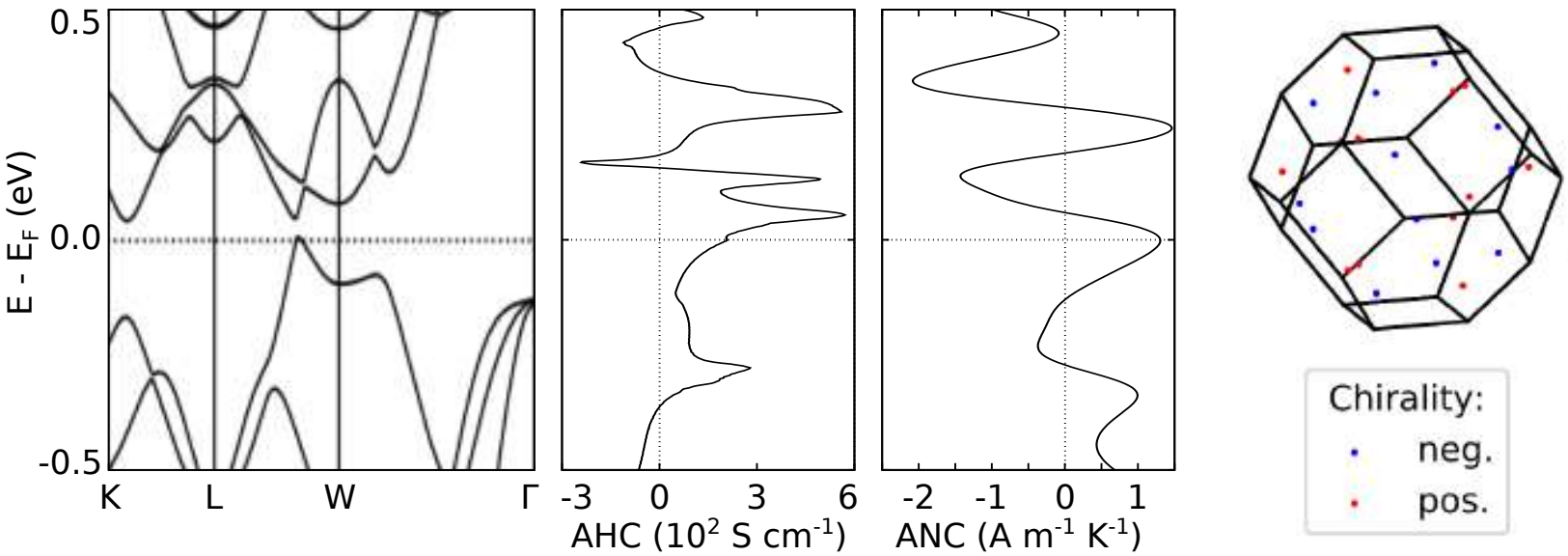

- Ferrimagnet with vanishing net magnetic moment
- Clean Fermi surface with Weyl points slightly above
- Peak in the AHC at Weyl point energy
- Large ANC around E_F

[6] JN *et al.*, Physical Review B 97, 220405(R) (2018)

Anomalous transport in topological metals

Model for a nodal line gapping

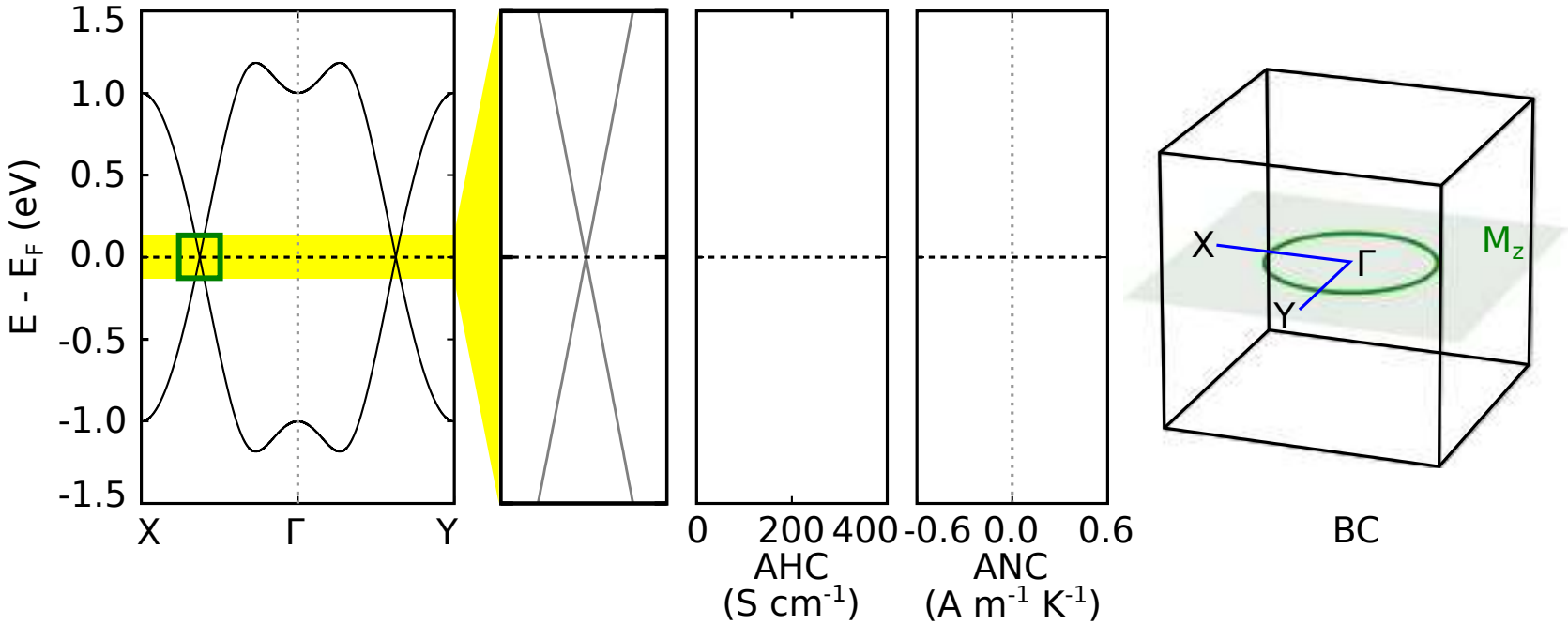

- Model from Rauch *et al.*[7]: nodal line at E_F in k_x-k_y plane is protected by a mirror symmetry

[7] T. Rauch *et al.*, Physical Review B **96**, 235103 (2017)

Anomalous transport in topological metals

Model for a nodal line gapping

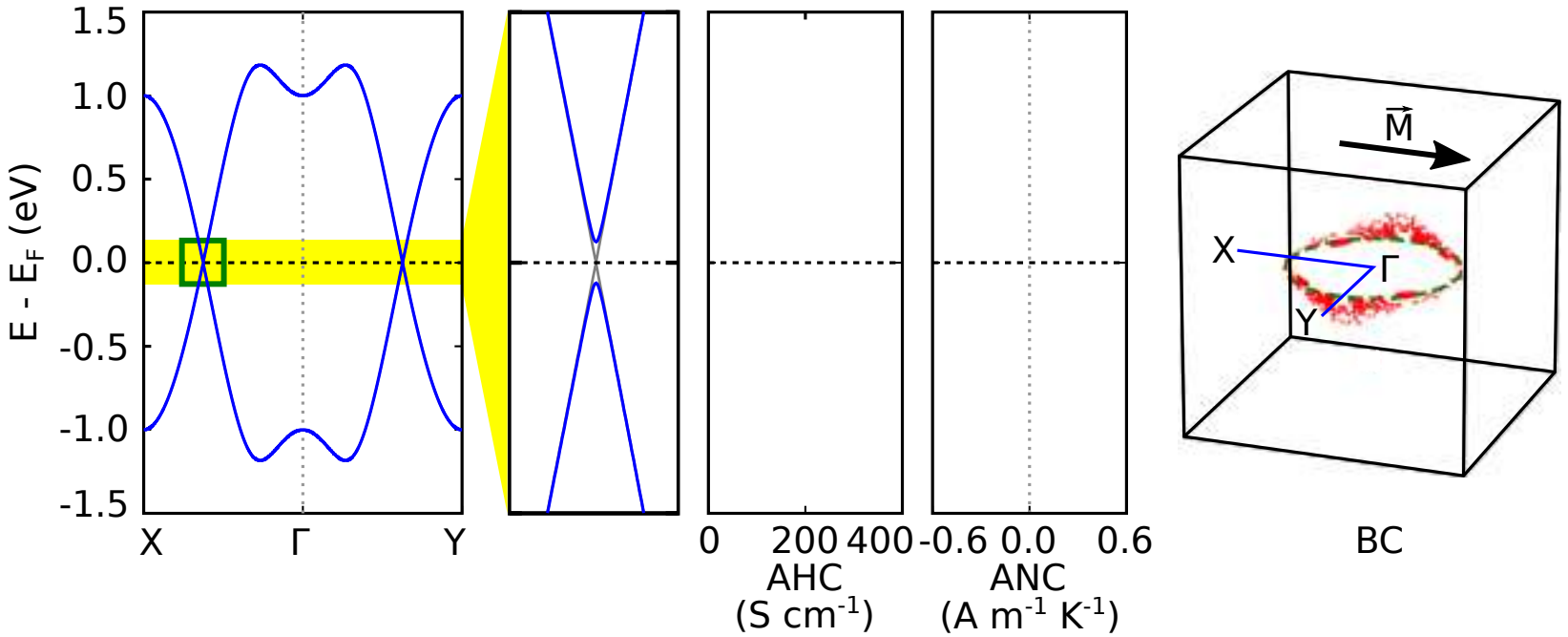

- Model from Rauch *et al.*[7]: nodal line at E_F in k_x-k_y plane is protected by a mirror symmetry
- Nodal line gapped $\rightarrow$ strong BC

[7] T. Rauch *et al.*, Physical Review B **96**, 235103 (2017)

Anomalous transport in topological metals

Model for a nodal line gapping

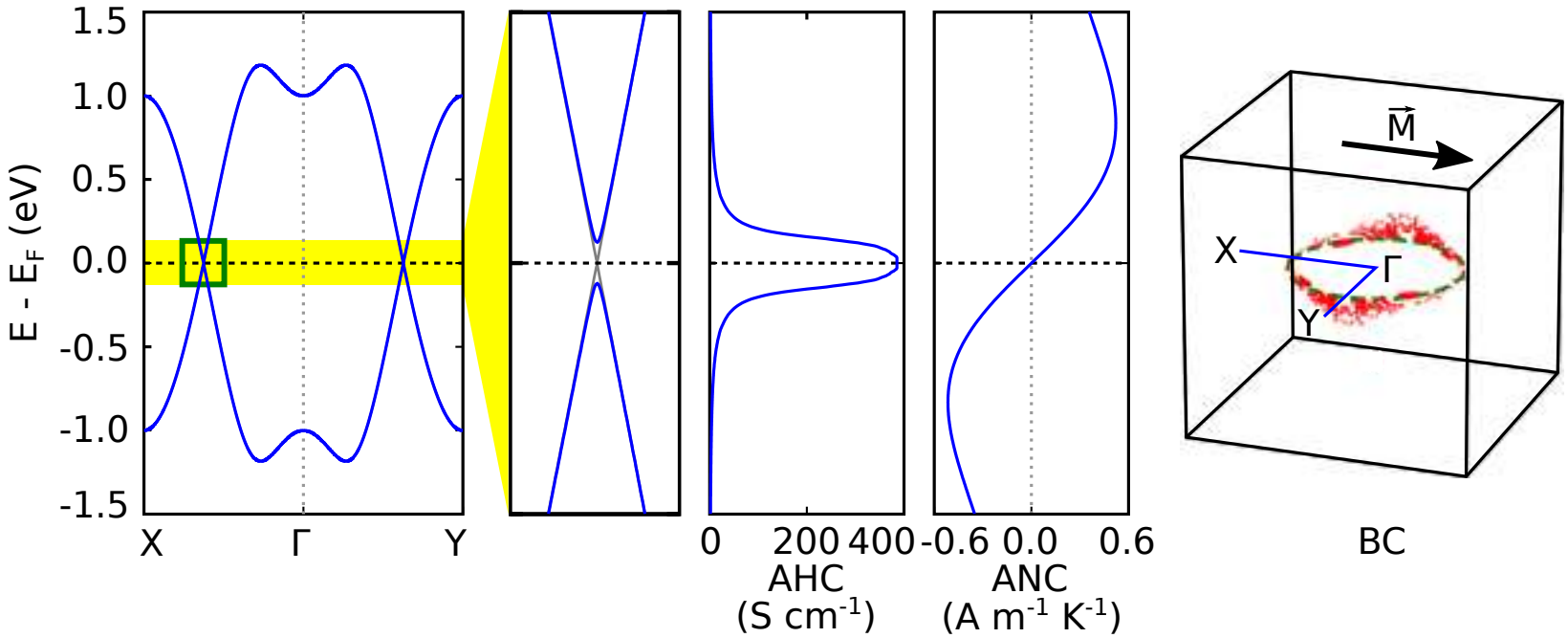

- Model from Rauch *et al.*[7]: nodal line at E_F in k_x-k_y plane is protected by a mirror symmetry
- Nodal line gapped $\rightarrow$ strong BC $\rightarrow$ strong AHC and ANC[8]

[7] T. Rauch *et al.*, Physical Review B **96**, 235103 (2017)
[8] JN *et al.*, Physical Review B 99, 165117 (2019)

Anomalous transport in topological metals

Co_2MnGa - nodal lines at the Fermi level

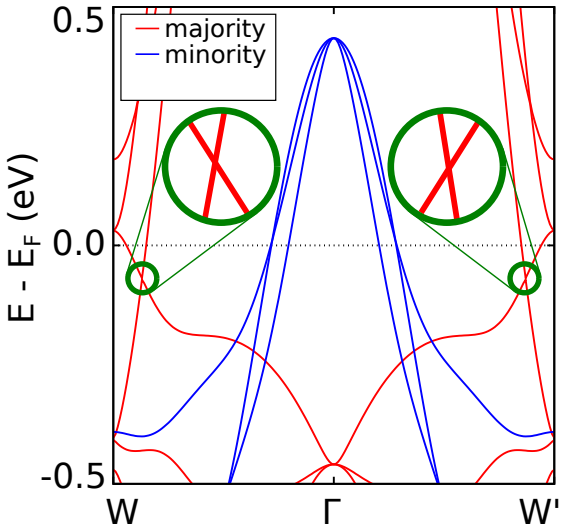

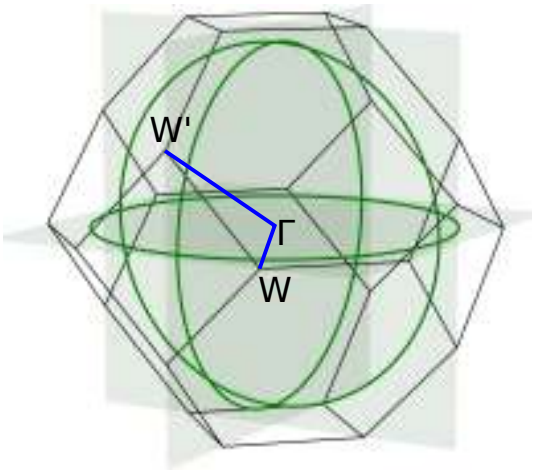

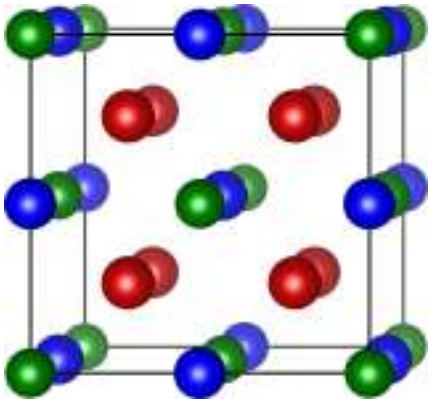

- Without SOC: 3 mirror planes $\rightarrow$ 3 nodal lines near E_F

[2] S. Guin, ..., JN *et al.*, NPG Asia Materials 11, 16 (2019)

Anomalous transport in topological metals

Co_2MnGa - nodal lines at the Fermi level

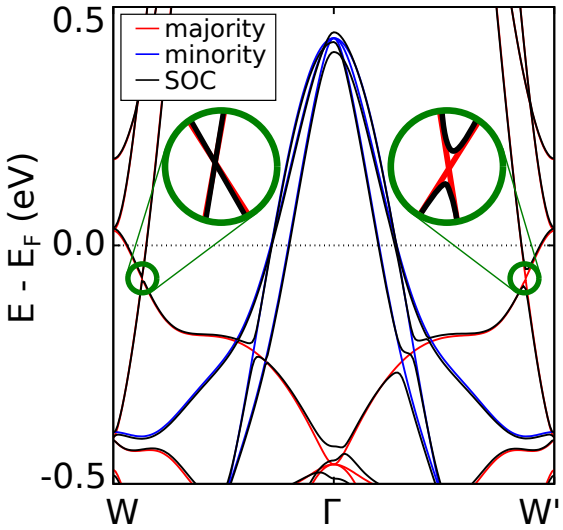

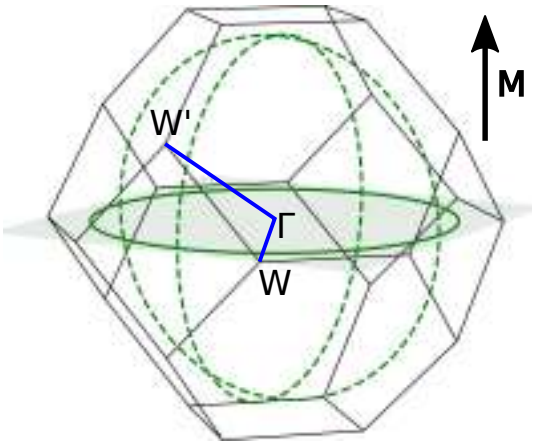

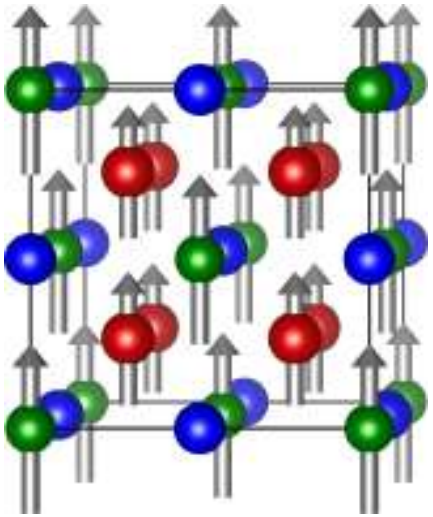

- Without SOC: 3 mirror planes $\rightarrow$ 3 nodal lines near E_F
- With SOC and $\vec{M}||001$: 2 mirrors broken

[2] S. Guin, ..., JN *et al.*, NPG Asia Materials 11, 16 (2019)

Anomalous transport in topological metals

Co_2MnGa - nodal lines at the Fermi level

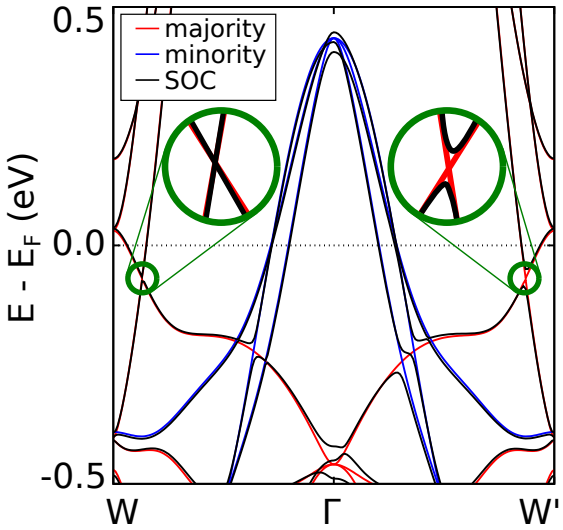

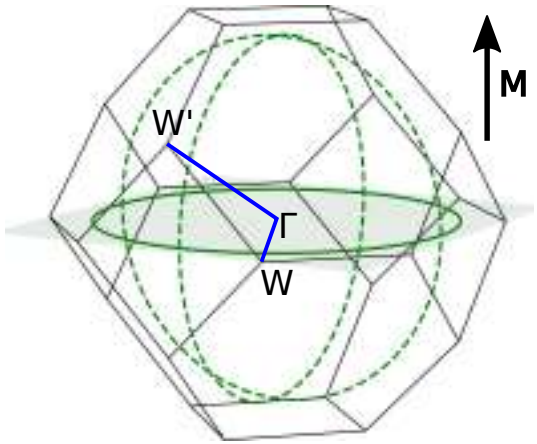

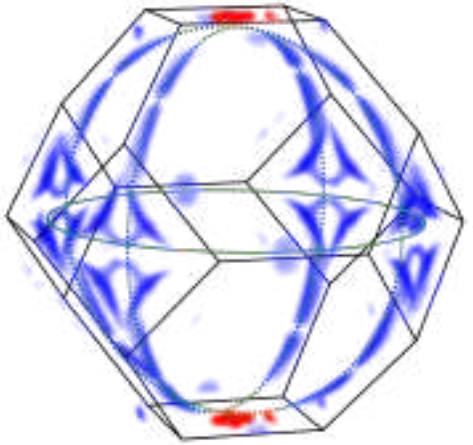

- Without SOC: 3 mirror planes $\rightarrow$ 3 nodal lines near E_F
- With SOC and $\vec{M}||001$: 2 mirrors broken
- Gapped lines induce strong Berry curvature

[2] S. Guin, ..., JN *et al.*, NPG Asia Materials 11, 16 (2019)

Anomalous transport in topological metals

Co_2MnGa - nodal lines at the Fermi level

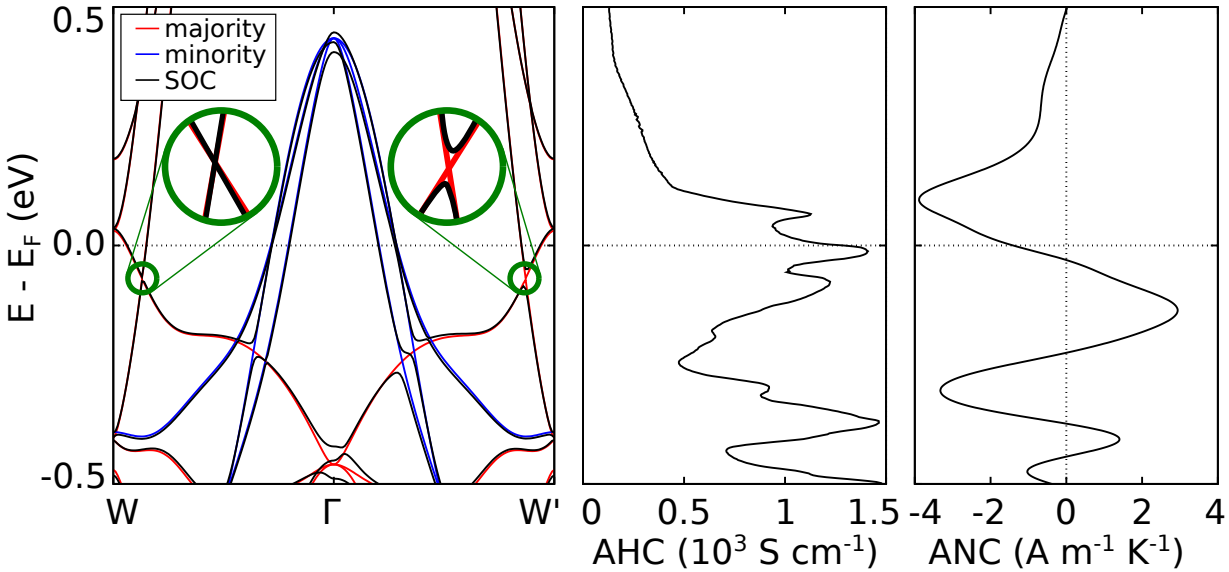

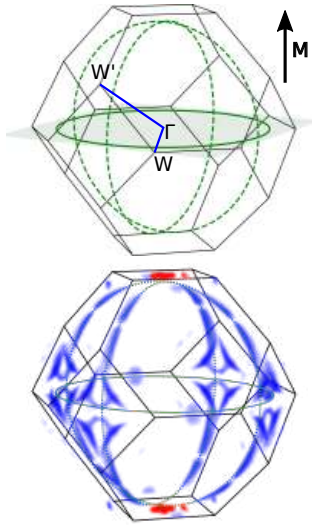

- Without SOC: 3 mirror planes $\rightarrow$ 3 nodal lines near E_F
- With SOC and $\vec{M}||001$: 2 mirrors broken
- Gapped lines induce strong Berry curvature
- High AHE at E_F, strong ANE near the nodal line

[2] S. Guin, ..., JN *et al.*, NPG Asia Materials 11, 16 (2019)

Anomalous transport in topological metals

Model for a nodal line away from the Fermi level

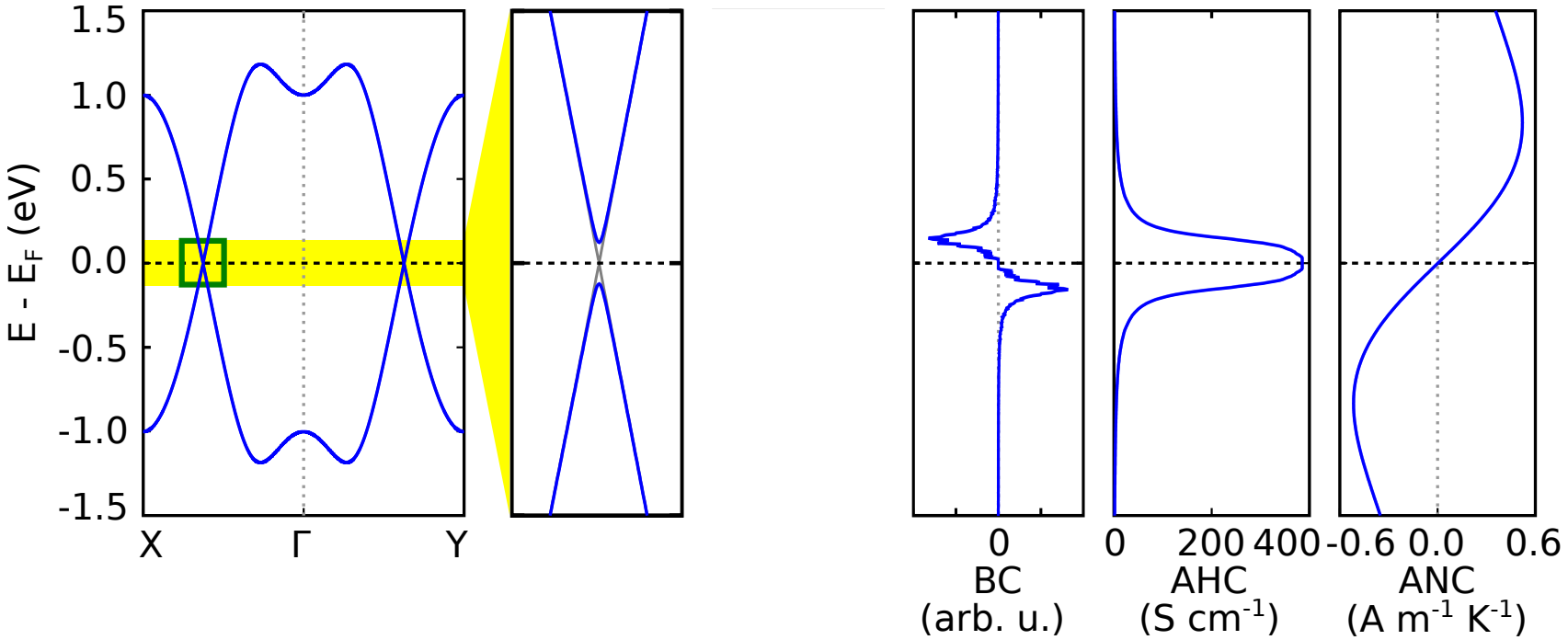

Anomalous transport in topological metals

Model for a nodal line away from the Fermi level

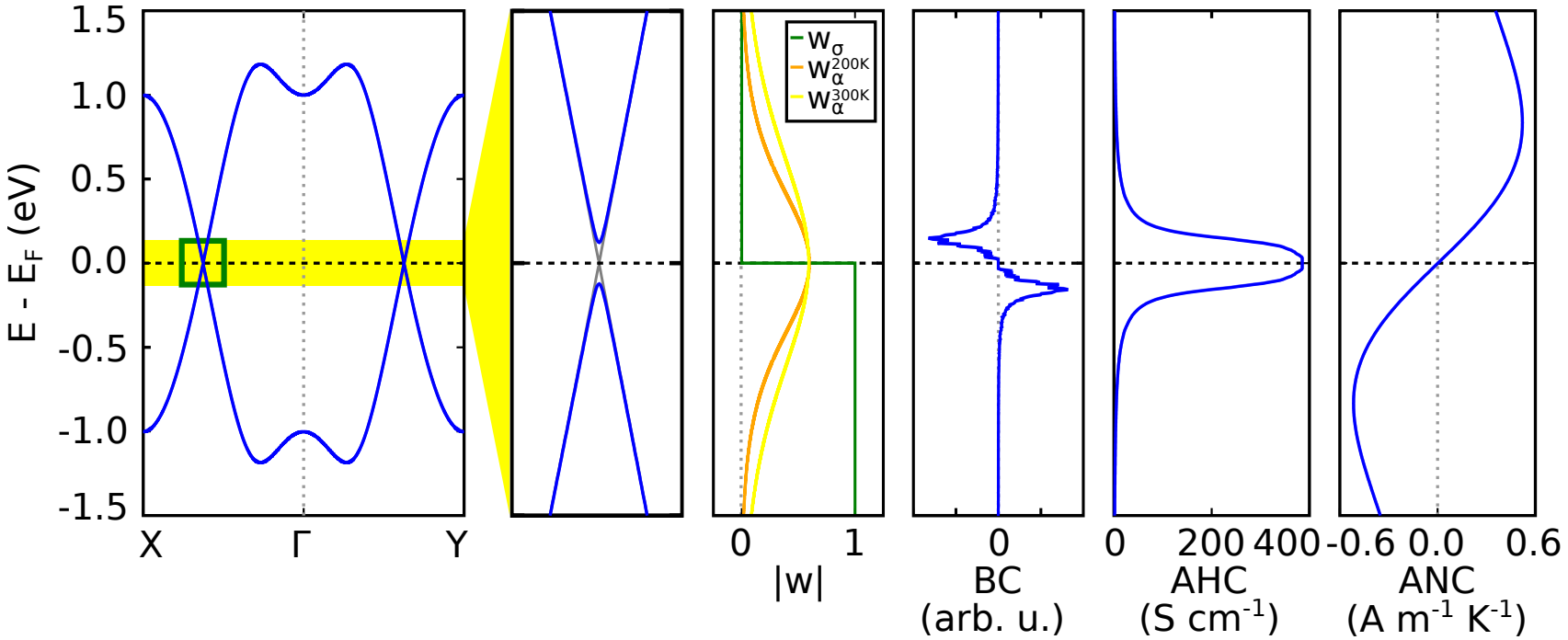

$$\sigma_{ij} = \frac{e^2}{\hbar} \sum_n \int \frac{d^3k}{(2\pi)^3} \Omega_{ij}^{n\mathbf{k}} f_{n\mathbf{k}}$$

$$\alpha_{ij} = \frac{e^2}{\hbar} \sum_n \int \frac{d^3k}{(2\pi)^3} \Omega_{ij}^{n\mathbf{k}} -\frac{1}{eT}[(E_{n\mathbf{k}} - E_F) f_{n\mathbf{k}} + k_B T \ln\left(1 + \exp \frac{E_{n\mathbf{k}} - E_F}{-k_B T}\right)]$$

[9] JN *et al.*, Physical Review B **98**, 241106(R) (2018)

Anomalous transport in topological metals

Model for a nodal line away from the Fermi level

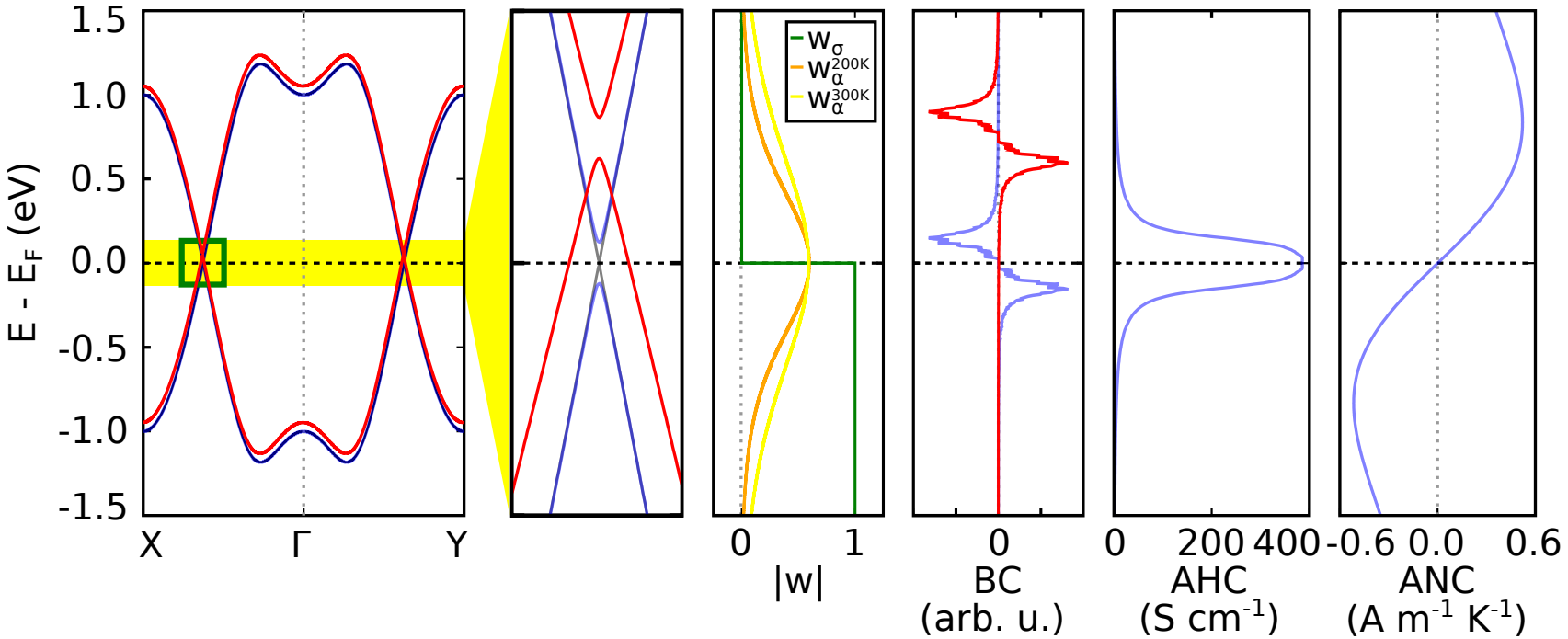

- BC contributes differently to AHE and ANE
- Now: shifting the nodal line away from the E_F

[9] JN *et al.*, Physical Review B **98**, 241106(R) (2018)

Anomalous transport in topological metals

Model for a nodal line away from the Fermi level

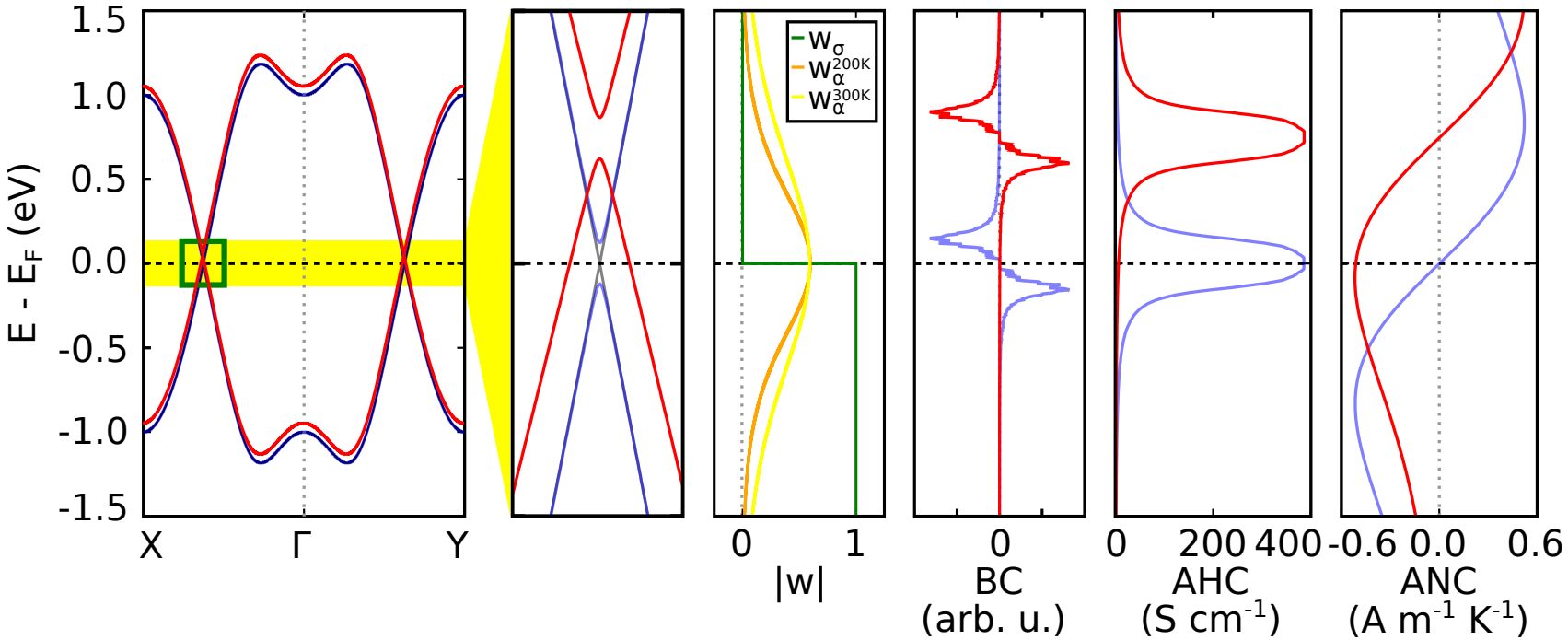

- BC contributes differently to AHE and ANE
- Now: shifting the nodal line away from the E_F
- AHC at the E_F vanishes but ANC is finite

[9] JN *et al.*, Physical Review B **98**, 241106(R) (2018)

Anomalous transport in topological metals

Co_2FeGe - nodal lines away from the Fermi level

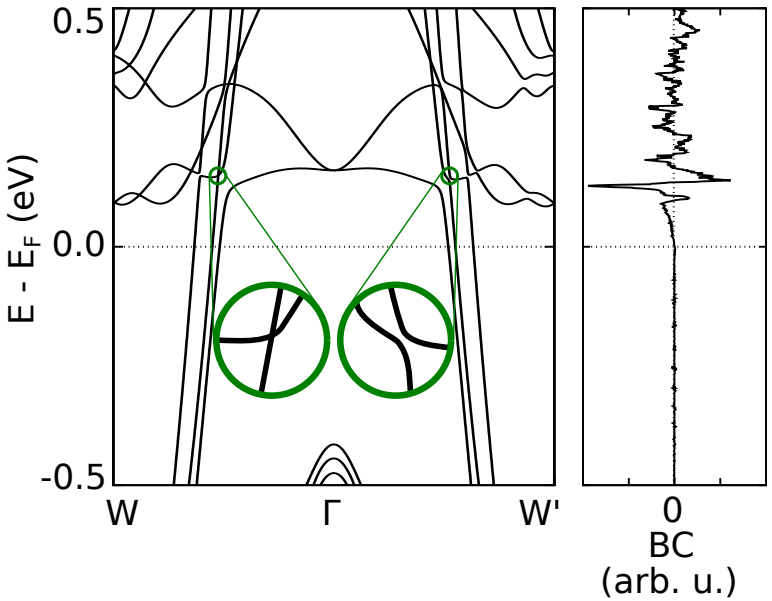

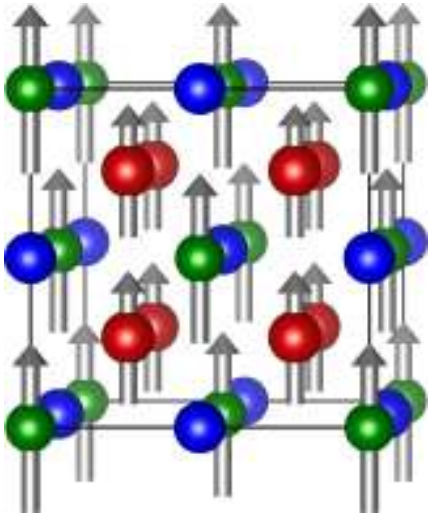

- Co_2FeGe: symmetries as in Co_2MnGa $\rightarrow$ same nodal line structure but: $\approx$ 100 meV above the E_F

[9] JN *et al.*, Physical Review B **98**, 241106(R) (2018)

Anomalous transport in topological metals

Co_2FeGe - nodal lines away from the Fermi level

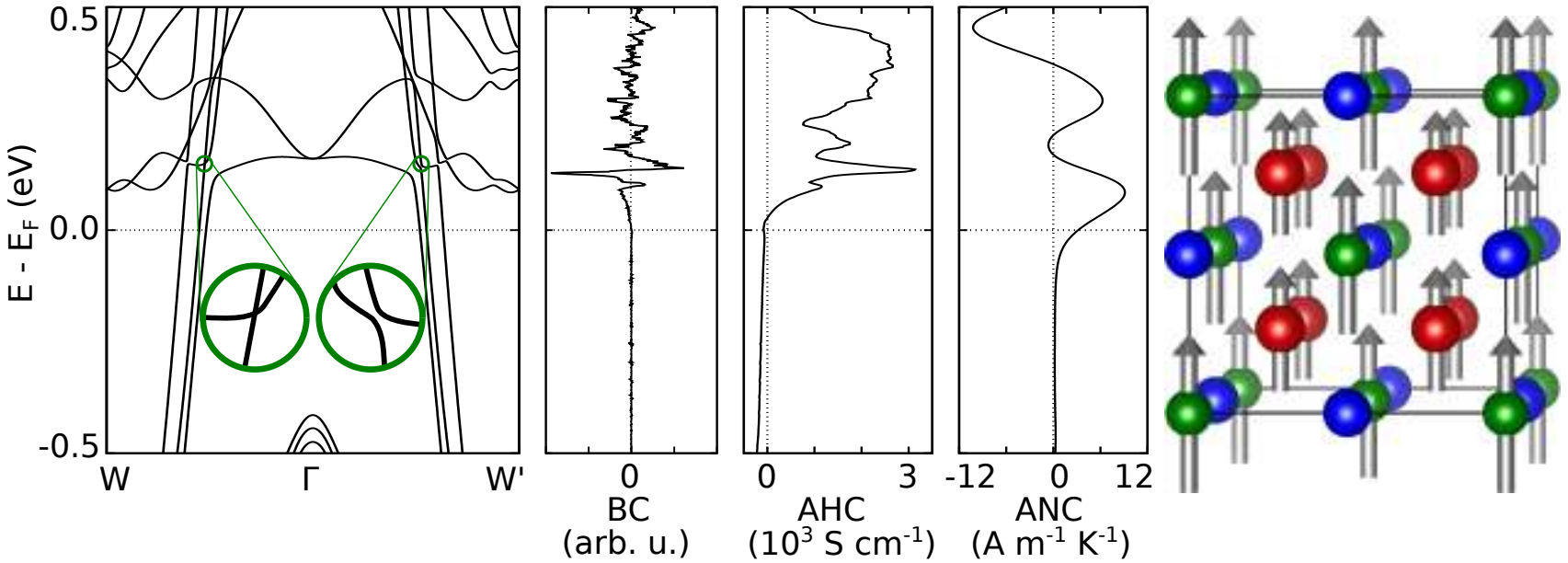

- Co_2FeGe: symmetries as in Co_2MnGa $\rightarrow$ same nodal line structure but: $\approx$ 100 meV above the E_F
- At E_F: AHC vanishes, ANC large (≈ 4 A m^{-1} K^{-1})

[9] JN *et al.*, Physical Review B **98**, 241106(R) (2018)

Anomalous transport in topological metals

Workflow

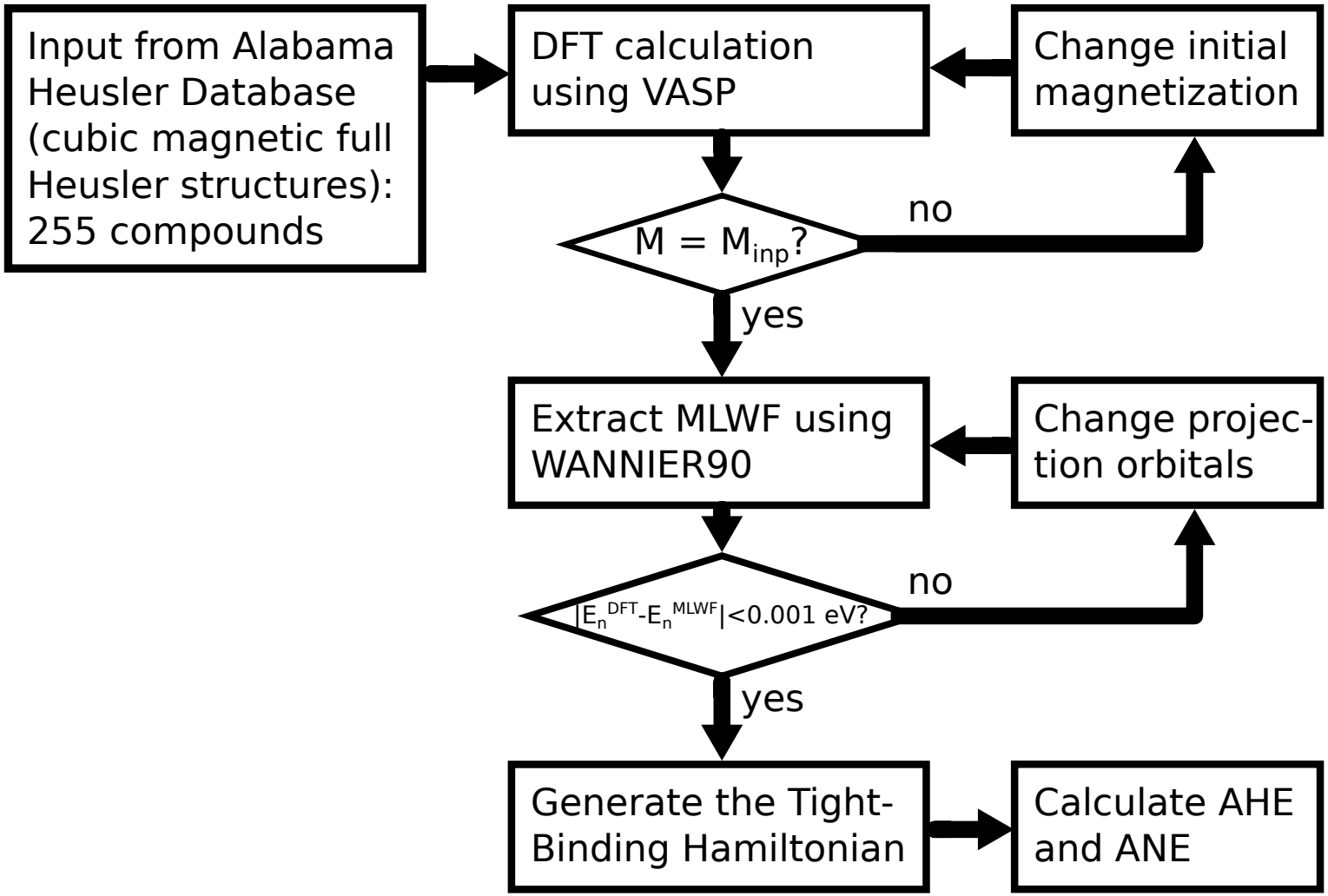

[10] Alabama Heusler Database (2015). URL http://heusleralloys.mint.ua.edu/

Anomalous transport in topological metals

Influence of the space group and mirror planes

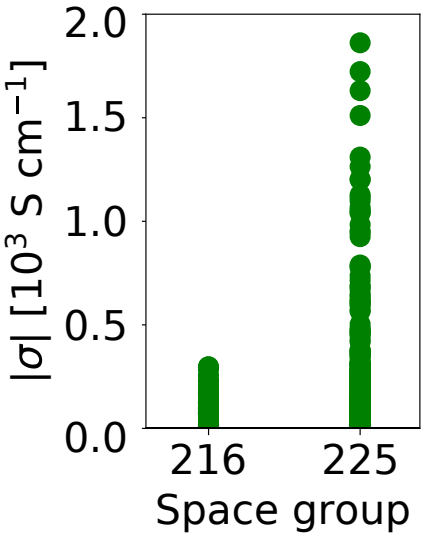

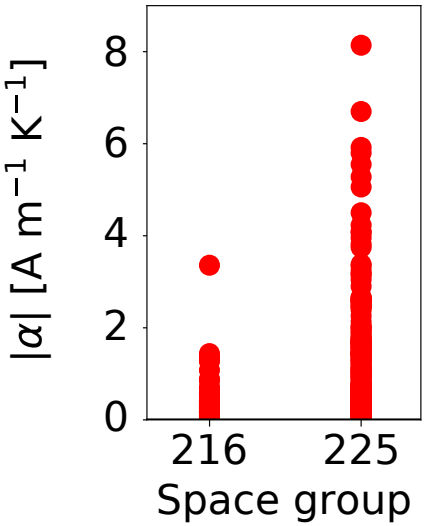

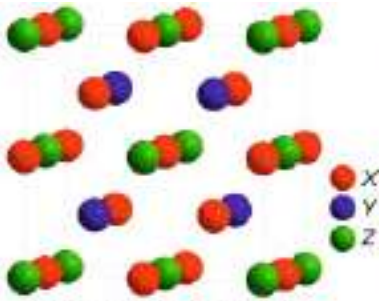

Inverse (SG 216)

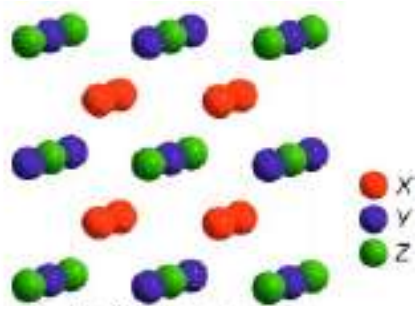

Regular (SG 225)

- Both effects larger in SG 225

[11] JN *et al.*, npj Computational Materials 6, 77 (2020)

Anomalous transport in topological metals

Influence of the space group and mirror planes

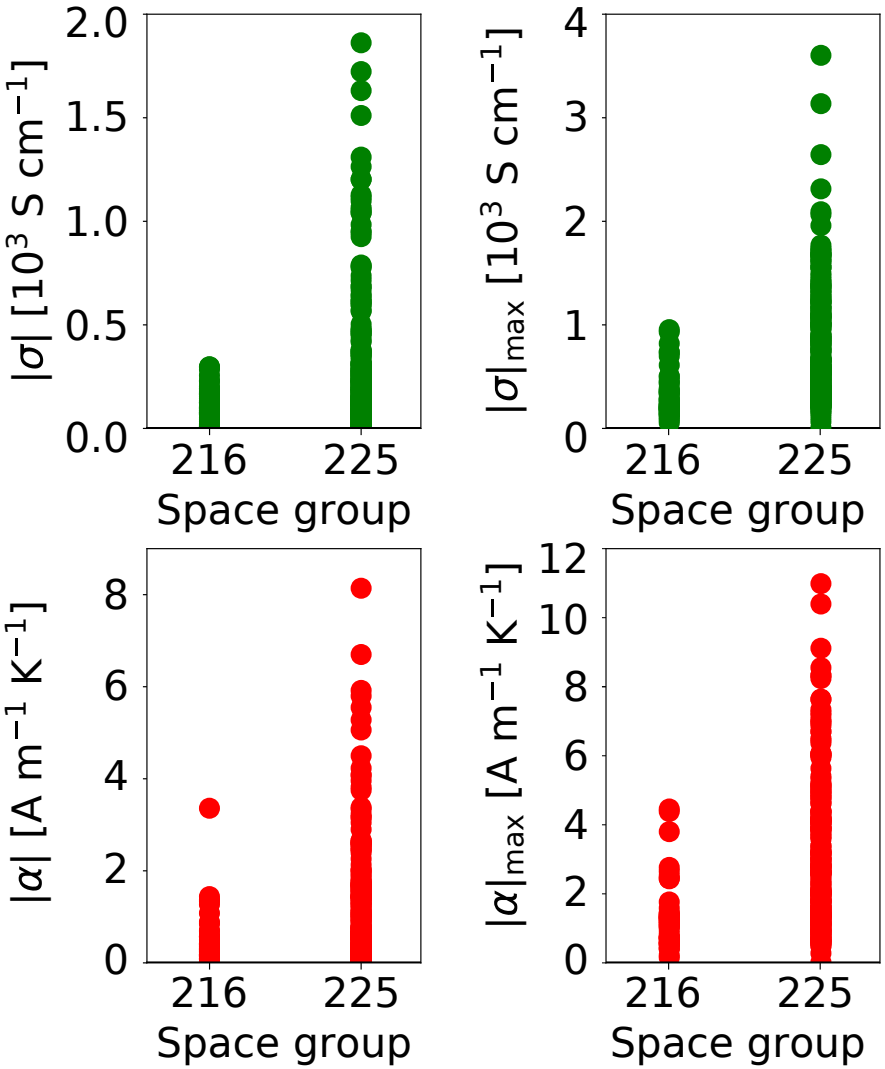

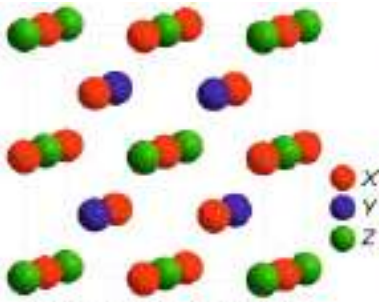

Inverse (SG 216)

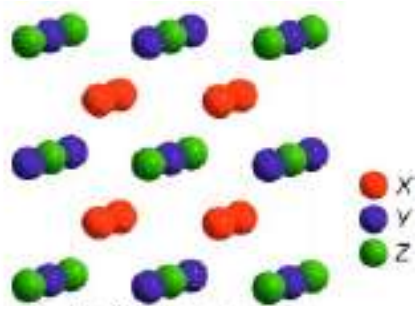

Regular (SG 225)

- Both effects larger in SG 225
- Maximum values larger in SG 225 (three additional mirrors)

[11] JN *et al.*, npj Computational Materials 6, 77 (2020)

Anomalous transport in topological metals

Influence of the space group and mirror planes

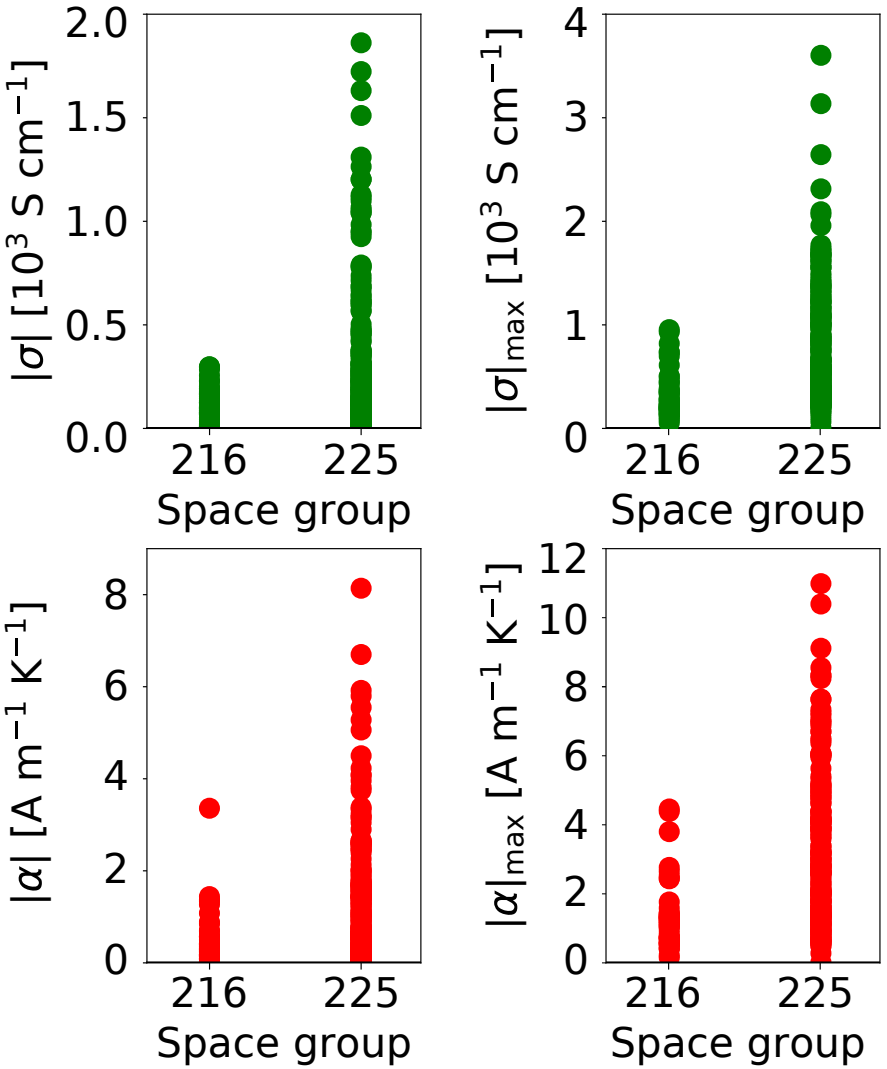

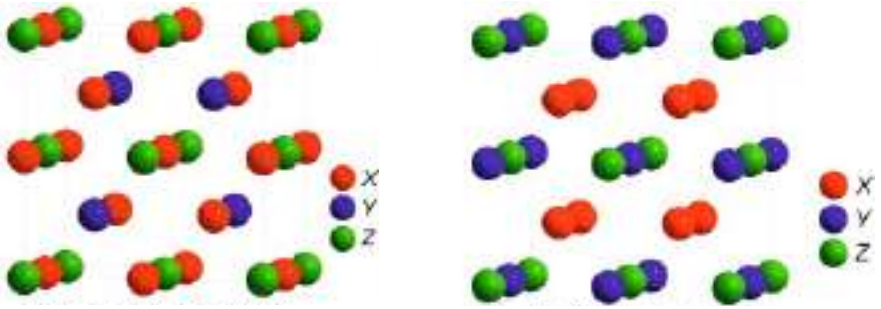

Inverse (SG 216) Regular (SG 225)

- Both effects larger in SG 225
- Maximum values larger in SG 225 (three additional mirrors)
- Effect can be understood from the nodal line model

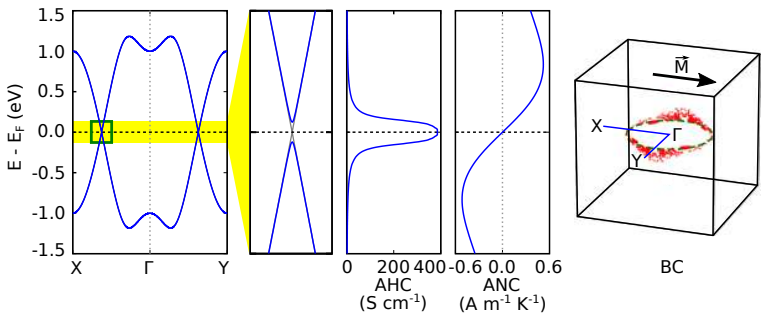

[11] JN *et al.*, npj Computational Materials 6, 77 (2020)

Anomalous transport in topological metals

Connections of the anomalous Hall and Nernst effects

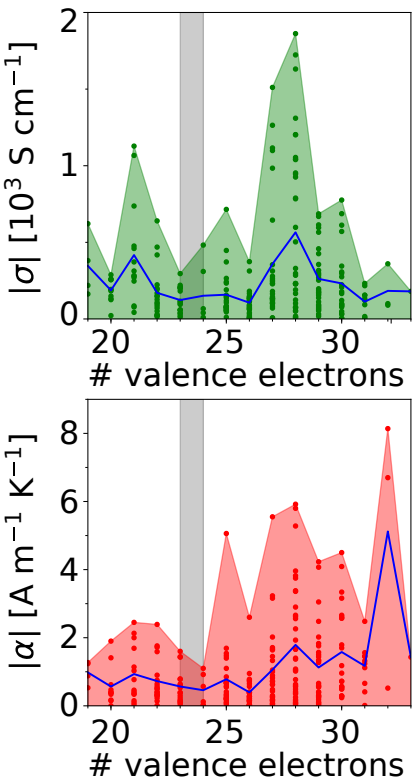

- Two peaks for AHE and ANE vs. valence electron number

[11] JN *et al.*, npj Computational Materials 6, 77 (2020)

Anomalous transport in topological metals

Connections of the anomalous Hall and Nernst effects

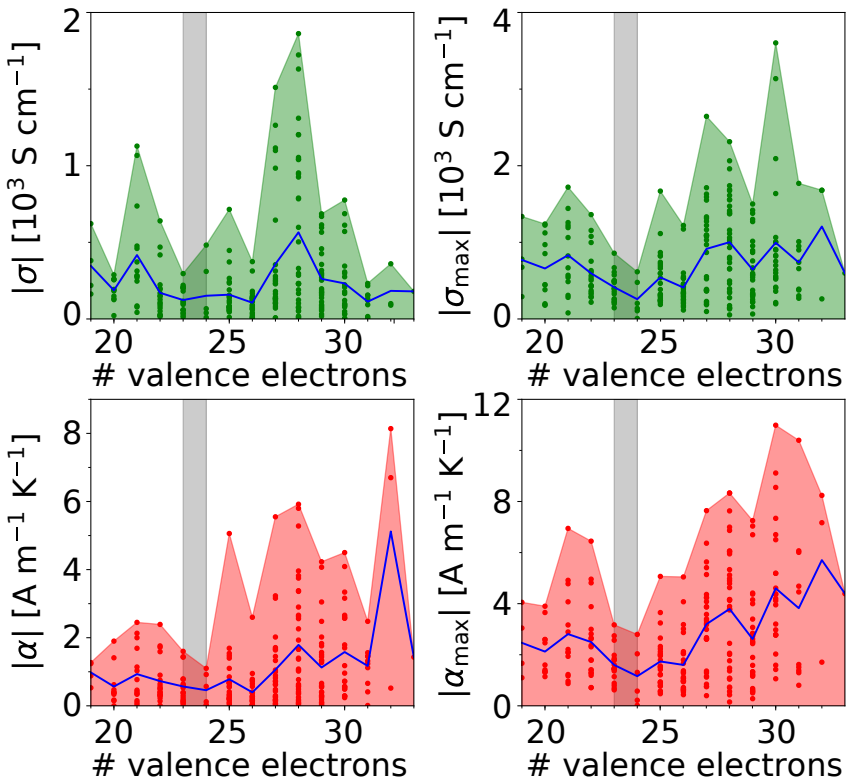

- Two peaks for AHE and ANE vs. valence electron number
- Band filling is important to bring E_F close to the nodal line

[11] JN *et al.*, npj Computational Materials 6, 77 (2020)

Anomalous transport in topological metals

Connections of the anomalous Hall and Nernst effects

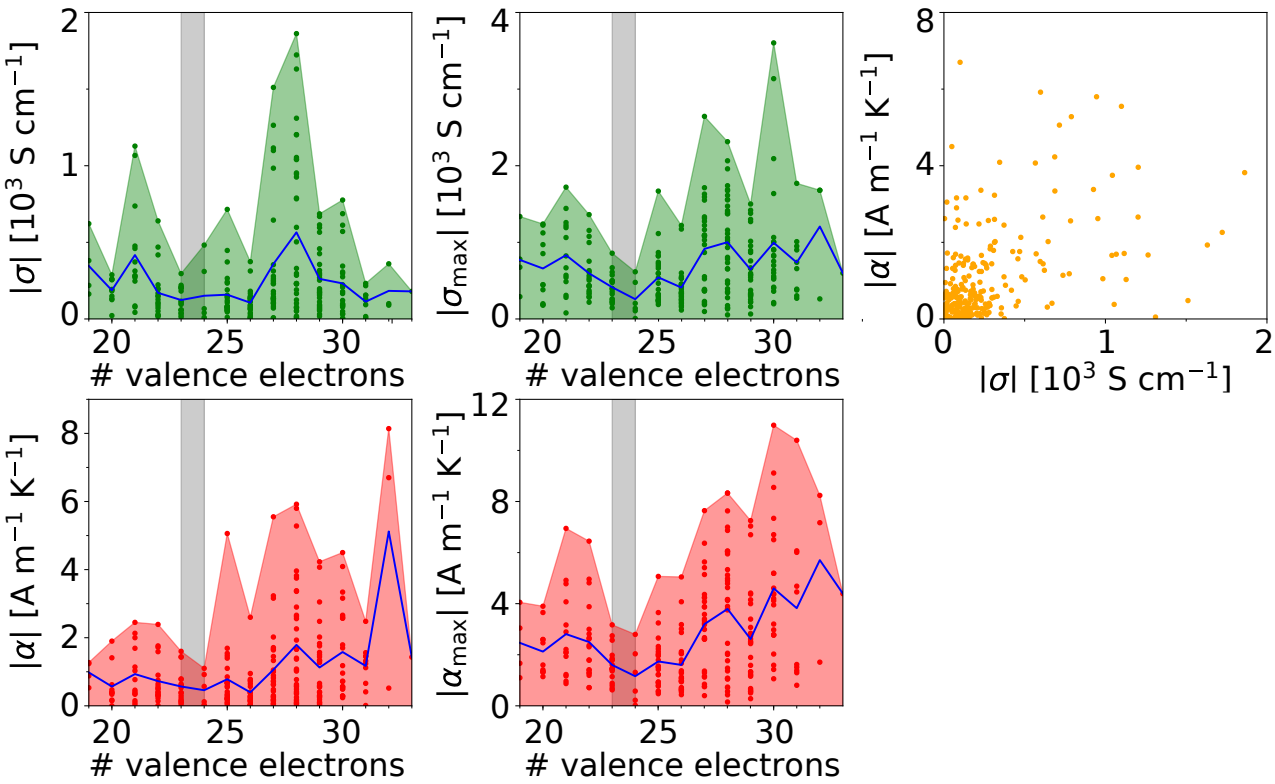

- Two peaks for AHE and ANE vs. valence electron number
- Band filling is important to bring E_F close to the nodal line
- No correlation between AHE and ANE

[11] JN *et al.*, npj Computational Materials 6, 77 (2020)

Anomalous transport in topological metals

Connections of the anomalous Hall and Nernst effects

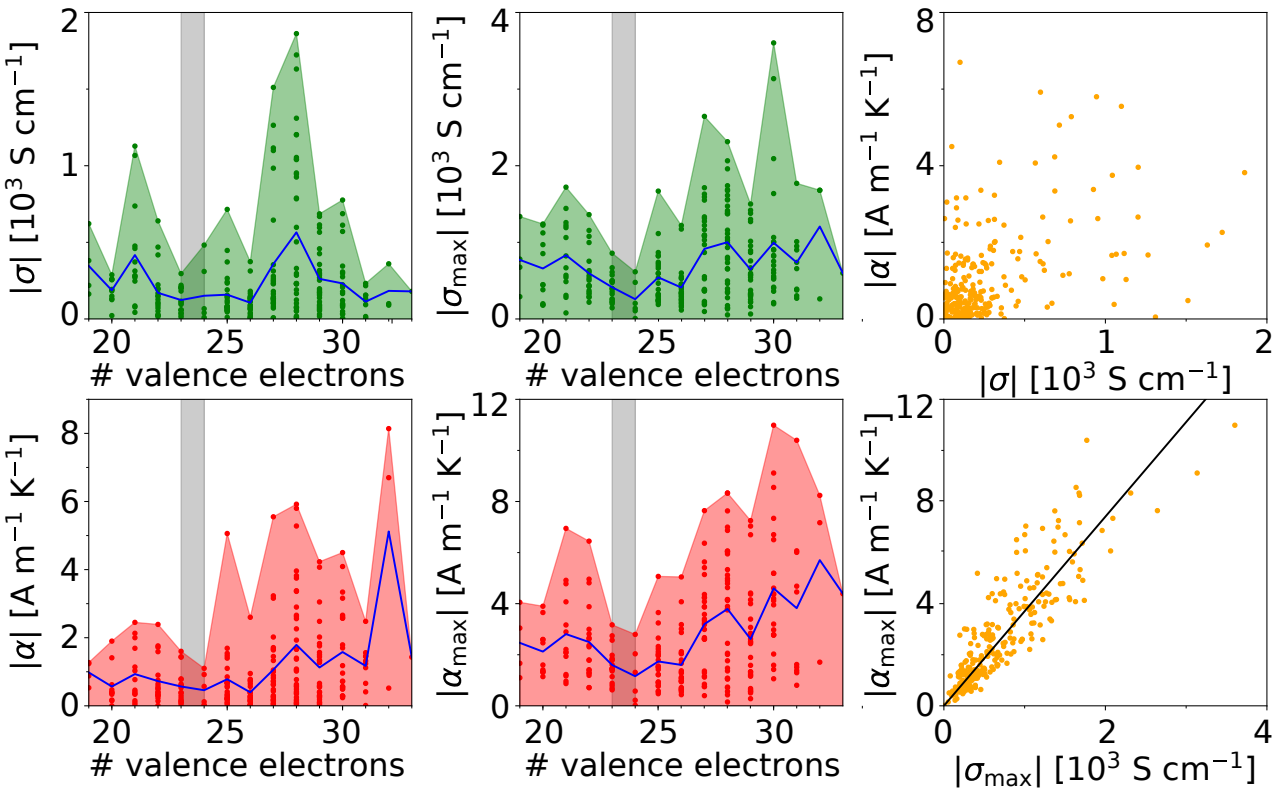

- Two peaks for AHE and ANE vs. valence electron number
- Band filling is important to bring E_F close to the nodal line
- No correlation between AHE and ANE but linear for maxima

[11] JN *et al.*, npj Computational Materials 6, 77 (2020)

Anomalous transport in topological metals

Table results

Material	SG	a_0 (Å)	μ (μ_B/f.u.)	AHC (S cm^{-1})	AHC$_{max}$ ($\Delta E/\Delta n$) (S cm^{-1})	ANC (A m^{-1} K^{-1})	ANC$_{max}$ ($\Delta E/\Delta n$) (A m^{-1} K^{-1})
Co_2MnAl	225	5.7	4.04	-1631	-1739 (-0.01/-0.02)	1.93	4.13 (0.04/0.05)
Co_2MnGa	225	5.72	4.11	-1310	-1473 (0.05/0.1)	-0.05	4.79 (0.09/0.17)
Fe_2MnP	225	5.55	4.0	-1202	-1373 (-0.04/-0.13)	2.66	7.63 (0.12/0.37)
Fe_2MnAs	225	5.7	4.02	-1043	-1413 (-0.06/-0.2)	3.75	7.0 (0.1/0.31)
Fe_2MnSb	225	5.95	4.11	-1203	-1374 (-0.06/-0.31)	3.96	-6.02 (-0.12/-0.67)
Rh_2MnAl	225	6.04	4.1	-1723	-2064 (-0.05/-0.13)	2.26	-6.06 (-0.12/-0.39)
Rh_2MnGa	225	6.06	4.13	-1862	-2313 (-0.04/-0.13)	3.82	-8.33 (-0.13/-0.45)
Rh_2CoAl	225	5.98	3.03	345	1005 (0.05/0.26)	4.09	-4.2 (0.12/0.57)
Rh_2NiSi	225	5.89	0.98	100	1678 (0.14/0.6)	6.7	7.17 (0.04/0.14)
Rh_2NiSn	225	6.21	1.0	360	1680 (0.11/0.55)	8.14	8.24 (0.01/0.04)
Ru_2MnP	225	5.91	3.95	-926	-1159 (0.03/0.08)	-3.38	-5.12 (-0.05/-0.15)
Ru_2FeP	225	5.9	4.13	-686	-1300 (0.04/0.17)	-4.23	-4.37 (-0.01/-0.05)
Ru_2FeAs	225	6.02	4.23	-566	-1378 (0.08/0.32)	-4.07	4.15 (0.16/0.74)

[11] JN *et al.*, npj Computational Materials 6, 77 (2020)

Anomalous transport in topological metals

Summary

Transport mechanisms

- Large BC in compensated collinear ferrimagnets possible
- Mirror-protected nodal lines and magnetism create large BC $\rightarrow$ enhancement of AHC and ANC
- Possibility for materials with no AHC but strong ANC

Anomalous transport in topological metals
Summary

Transport mechanisms

- Large BC in compensated collinear ferrimagnets possible
- Mirror-protected nodal lines and magnetism create large BC $\rightarrow$ enhancement of AHC and ANC
- Possibility for materials with no AHC but strong ANC

Heusler database calculation

- Mirror symmetries with magnetism can strongly enhance Berry curvature related effects
- No direct correlation of AHE and ANE $\rightarrow$ study separately
- Very large values for both AHE and ANE are possible

Anomalous transport in topological metals
Summary

Transport mechanisms

- Large BC in compensated collinear ferrimagnets possible
- Mirror-protected nodal lines and magnetism create large BC $\rightarrow$ enhancement of AHC and ANC
- Possibility for materials with no AHC but strong ANC

Heusler database calculation

- Mirror symmetries with magnetism can strongly enhance Berry curvature related effects
- No direct correlation of AHE and ANE $\rightarrow$ study separately
- Very large values for both AHE and ANE are possible

Thank you for your attention!

Appendix

- *ab-initio* band structure calculation using density-functional theory (DFT) as implemented in VASP (PP, PAW, PBE)
- Generate Maximally-localized Wannier functions from DFT using Wannier90 to extract tight-binding parameters

Berry curvature (BC) via the Kubo formalism

$$\Omega_{ij}^{n\mathbf{k}} = \sum_{m \neq n} \frac{\langle n\mathbf{k}|\frac{\partial H}{\partial k_i}|m\mathbf{k}\rangle\langle m\mathbf{k}|\frac{\partial H}{\partial k_j}|n\mathbf{k}\rangle - (i \leftrightarrow j)}{(E_{n\mathbf{k}} - E_{m\mathbf{k}})^2}$$

Anomalous Hall conductivity from BC

$$\sigma_{ij} = \frac{e^2}{\hbar} \sum_n \int \frac{d^3k}{(2\pi)^3} \Omega_{ij}^{n\mathbf{k}} f_{n\mathbf{k}}$$

Anomalous Nernst conductivity from BC

$$\alpha_{ij} = -\frac{1}{T}\frac{e}{\hbar} \sum_n \int \frac{d^3k}{(2\pi)^3} \Omega_{ij}^{n\mathbf{k}} [(E_{n\mathbf{k}} - E_F) f_{n\mathbf{k}} + k_B T \ln\left(1 + \exp\frac{E_{n\mathbf{k}} - E_F}{-k_B T}\right)]$$

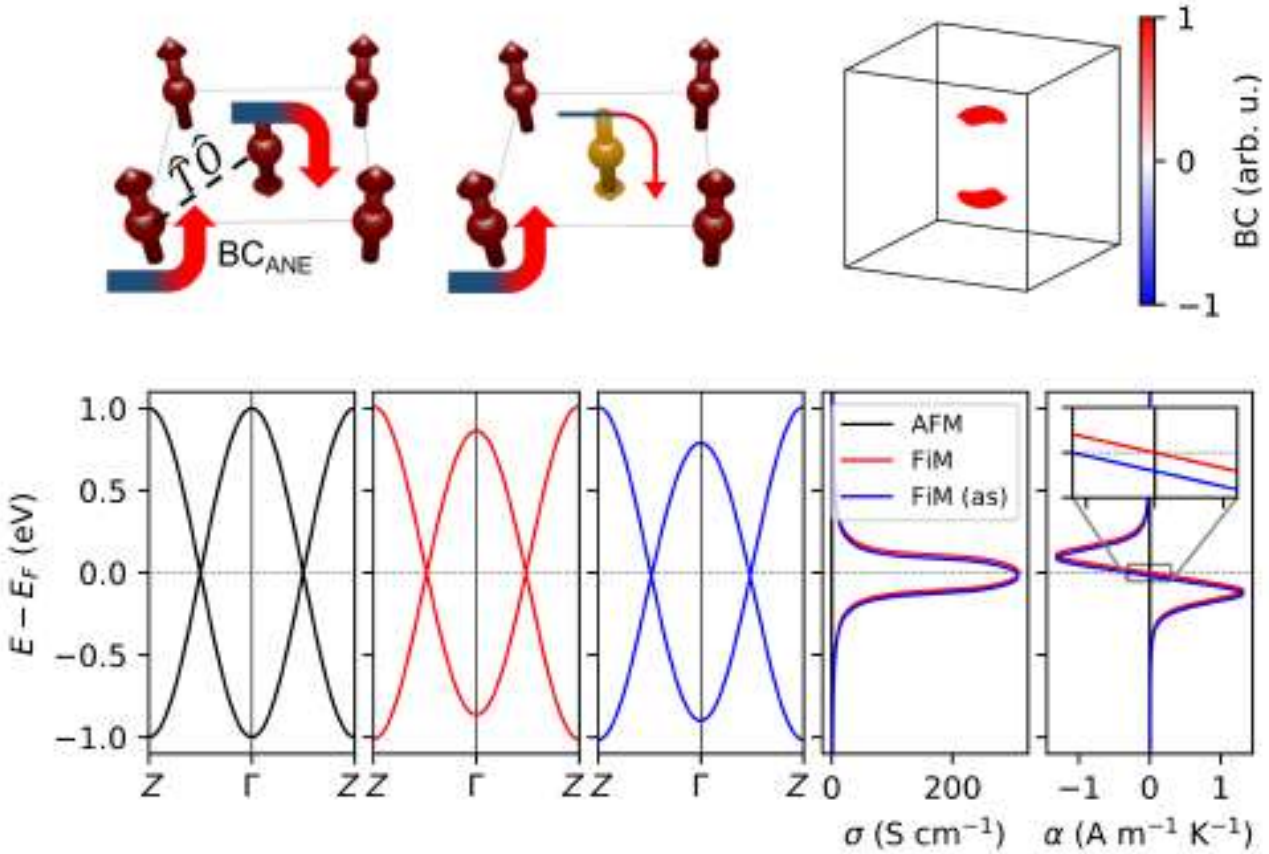

- AFM suppresses σ_{xy} and α_{xy} due to $\hat{T}\hat{O}$ symmetry
- Compensated FiM has no $\hat{T}\hat{O}$ symmetry $\rightarrow \sigma_{xy} \neq 0$
- Contributions mainly from the Weyl points

[9] JN *et al.*, Physical Review B 97, 220405(R) (2018)

$$H = (m - 6M + 2(\cos k_x + \cos k_y + \cos k_z))\tau_z \otimes \sigma_0 + \\ + B\tau_z \otimes \sigma_z + c \sin k_z \tau_x \otimes \sigma_z \\ + c \sin k_x \tau_x \otimes \sigma_x + c \sin k_y \tau_x \otimes \sigma_y$$

$$m = M = c = 1 \text{ eV and } B = 2 \text{ eV}$$

$$H^{break} = \lambda c(\sin k_x \tau_x \otimes \sigma_x + \sin k_z \tau_x \otimes \sigma_y)$$

$$\lambda = 0.01$$

$$H^{shift} = d\tau_0 \otimes \sigma_0$$

$$d = 0.1 \text{ eV}$$

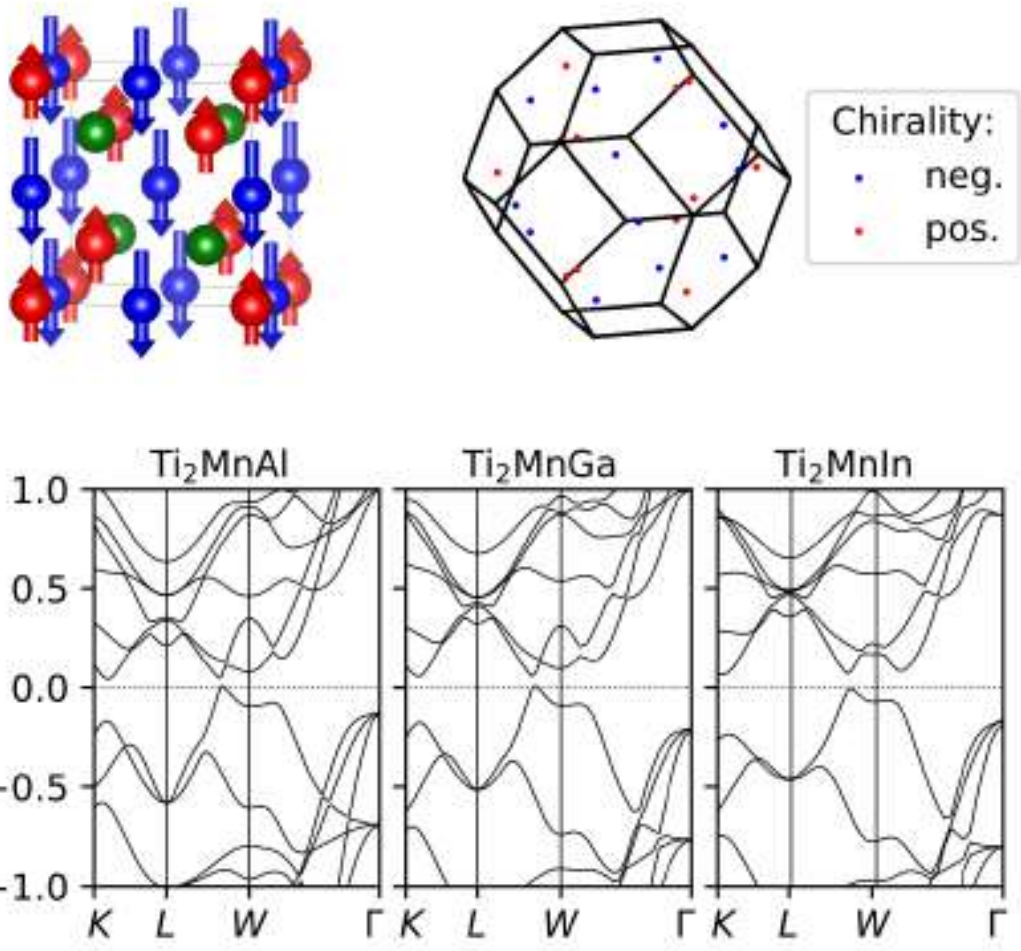

- Ti_2MnX (X = Al, Ga, In: inverse Heusler compounds
- Compensated FiM with Weyl points close to E_F

[9] JN *et al.*, Physical Review B 97, 220405(R) (2018)

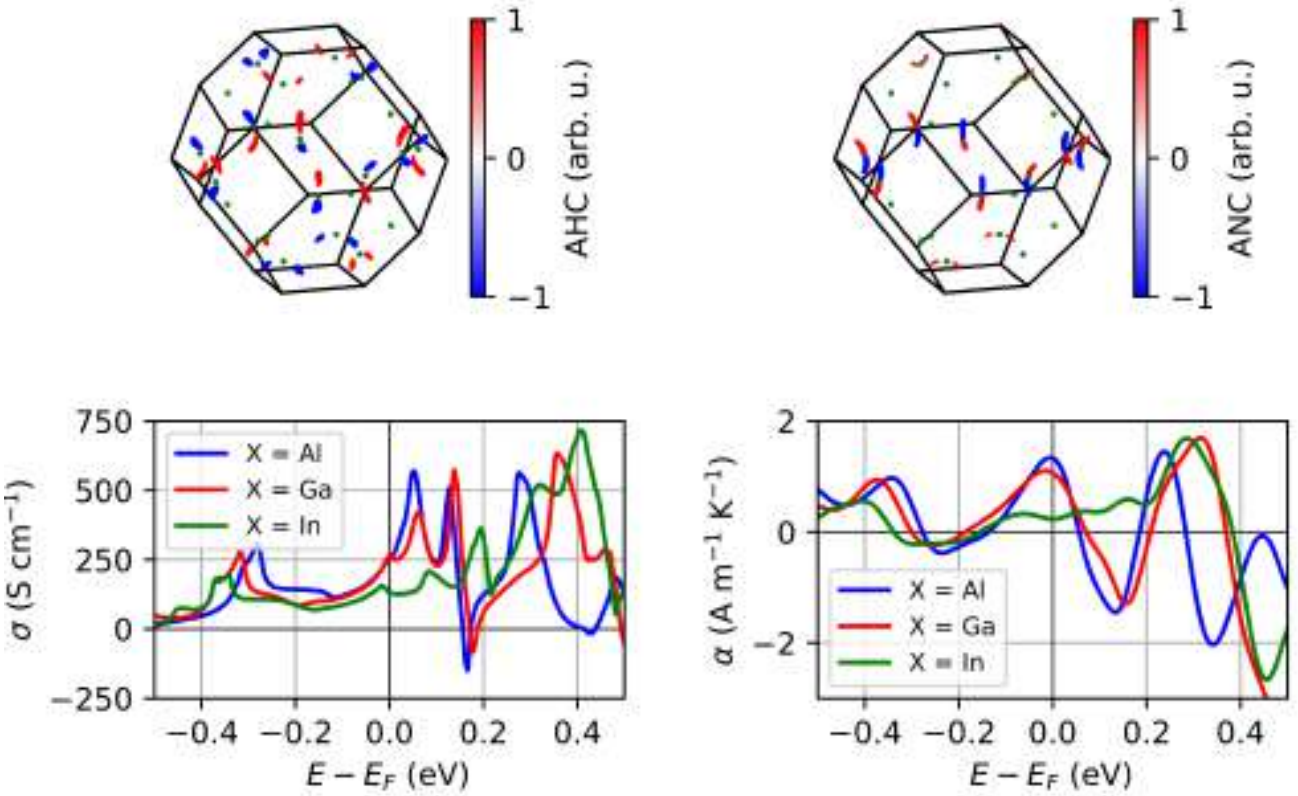

- Strong AHE and ANE in all three compounds
- Contributions mainly around the Weyl points in the Brillouin zone

[9] JN *et al.*, Physical Review B 97, 220405(R) (2018)

Anomalous transport in topological metals

Fe_2MnX - nodal line gapping

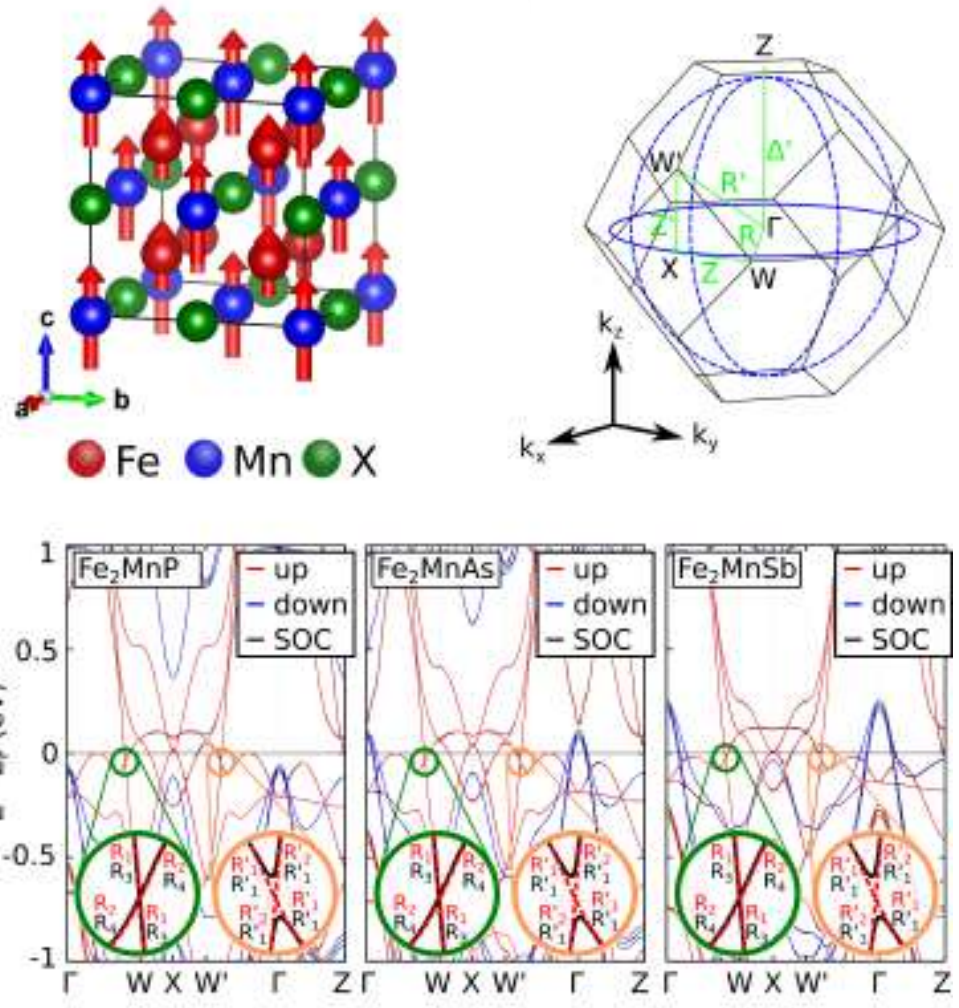

[10] JN *et al.*, Physical Review B 99, 165117 (2019)

Anomalous transport in topological metals

Influence of the magnetization direction

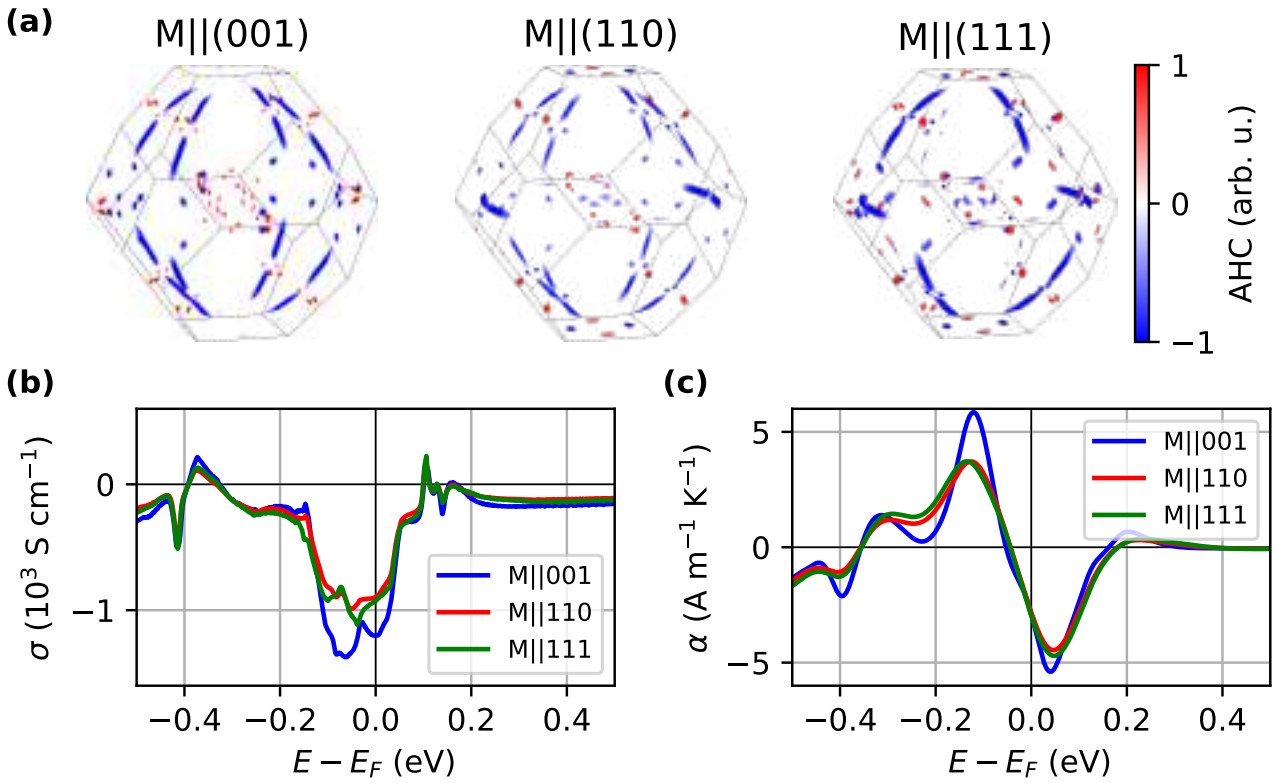

- Magnetization direction changes local BC but not overall AHC and ANC due to the high symmetry

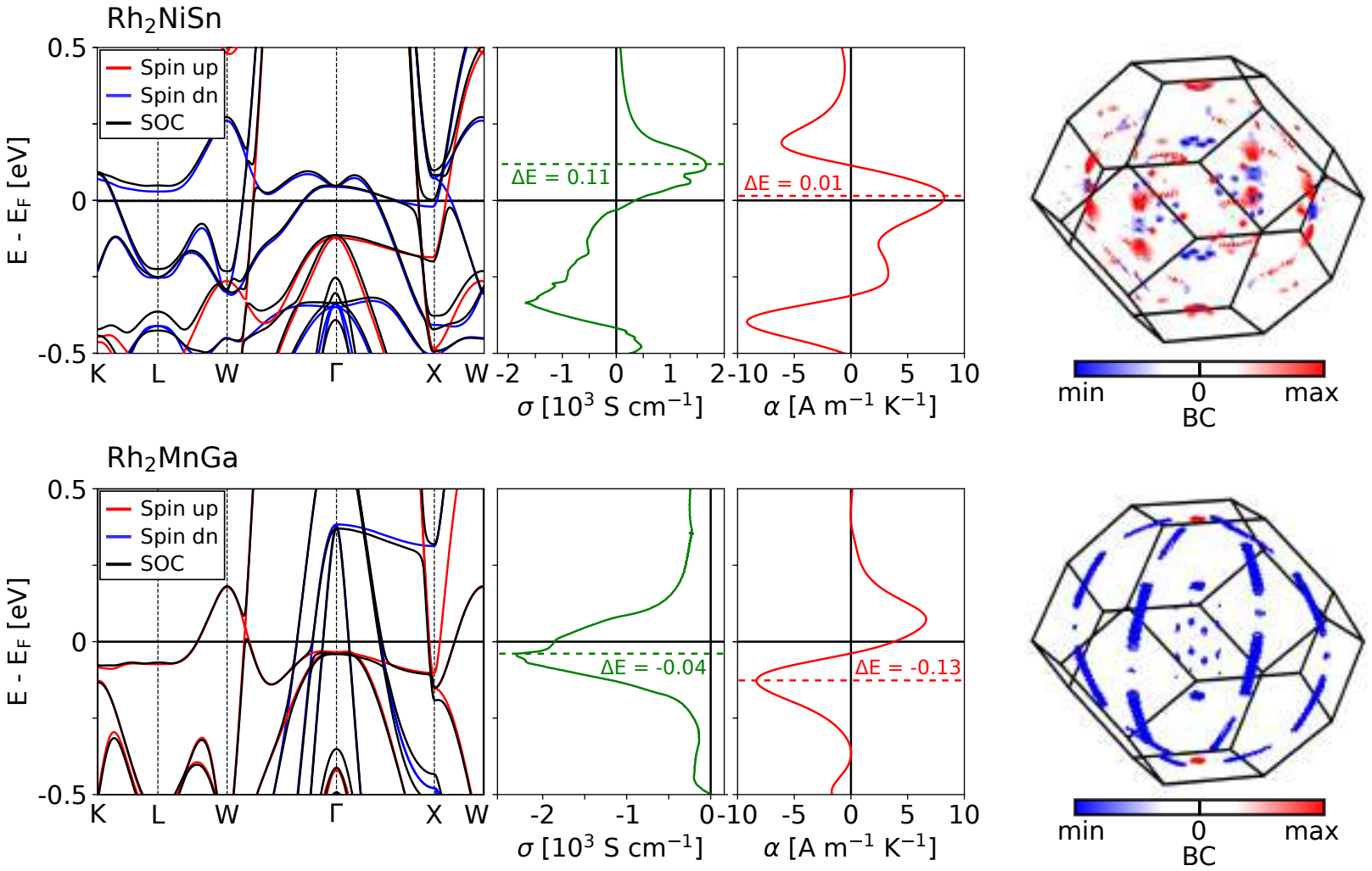

[8] JN *et al.*, npj Computational Materials 6, 77 (2020)

Anomalous transport in topological metals

Table results

Material	SG	a_0 (Å)	μ (μ_B/f.u.)	AHC (S cm^{-1})	AHC$_{max}$ ($\Delta E/\Delta n$) (S cm^{-1})	ANC (A m^{-1} K^{-1})	ANC$_{max}$ ($\Delta E/\Delta n$) (A m^{-1} K^{-1})
Co_2CrAl	225	5.7	3.0	-313	-1089 (-0.04/-0.24)	3.23	3.23 (0.0/-0.03)
Co_2MnAl	225	5.7	4.04	-1631	-1739 (-0.01/-0.02)	1.93	4.13 (0.04/0.05)
Co_2MnGa	225	5.72	4.11	-1310	-1473 (0.05/0.1)	-0.05	4.79 (0.09/0.17)
Co_2FeSi	225	5.63	5.4	-275	2092 (0.12/0.8)	2.57	7.34 (0.08/0.49)
Co_2FeGe	225	5.74	5.57	-78	3136 (0.14/0.84)	3.16	9.11 (0.08/0.43)
Co_2FeSn	225	5.99	5.6	49	3602 (0.12/0.85)	4.5	10.99 (0.07/0.4)
Fe_2MnP	225	5.55	4.0	-1202	-1373 (-0.04/-0.13)	2.66	7.63 (0.12/0.37)
Fe_2MnAs	225	5.7	4.02	-1043	-1413 (-0.06/-0.2)	3.75	7.0 (0.1/0.31)
Fe_2MnSb	225	5.95	4.11	-1203	-1374 (-0.06/-0.31)	3.96	-6.02 (-0.12/-0.67)
Rh_2MnAl	225	6.04	4.1	-1723	-2064 (-0.05/-0.13)	2.26	-6.06 (-0.12/-0.39)
Rh_2MnGa	225	6.06	4.13	-1862	-2313 (-0.04/-0.13)	3.82	-8.33 (-0.13/-0.45)
Rh_2FeIn	225	6.27	4.2	-18	1270 (0.12/0.63)	3.05	4.42 (0.07/0.33)
Rh_2CoAl	225	5.98	3.03	345	1005 (0.05/0.26)	4.09	-4.2 (0.12/0.57)
Rh_2NiSi	225	5.89	0.98	100	1678 (0.14/0.6)	6.7	7.17 (0.04/0.14)
Rh_2NiSn	225	6.21	1.0	360	1680 (0.11/0.55)	8.14	8.24 (0.01/0.04)
Ru_2MnP	225	5.91	3.95	-926	-1159 (0.03/0.08)	-3.38	-5.12 (-0.05/-0.15)
Ru_2FeP	225	5.9	4.13	-686	-1300 (0.04/0.17)	-4.23	-4.37 (-0.01/-0.05)
Ru_2FeAs	225	6.02	4.23	-566	-1378 (0.08/0.32)	-4.07	4.15 (0.16/0.74)
Ru_2CoGe	225	5.96	1.99	-138	-1500 (0.15/0.91)	-2.48	-6.7 (0.11/0.68)
Ru_2CoP	225	5.84	2.18	-776	-899 (-0.03/-0.14)	1.18	-6.5 (-0.12/-0.62)

[8] JN *et al.*, npj Computational Materials 6, 77 (2020)

Anomalous transport in topological metals

2D free electron gas with external magnetic field

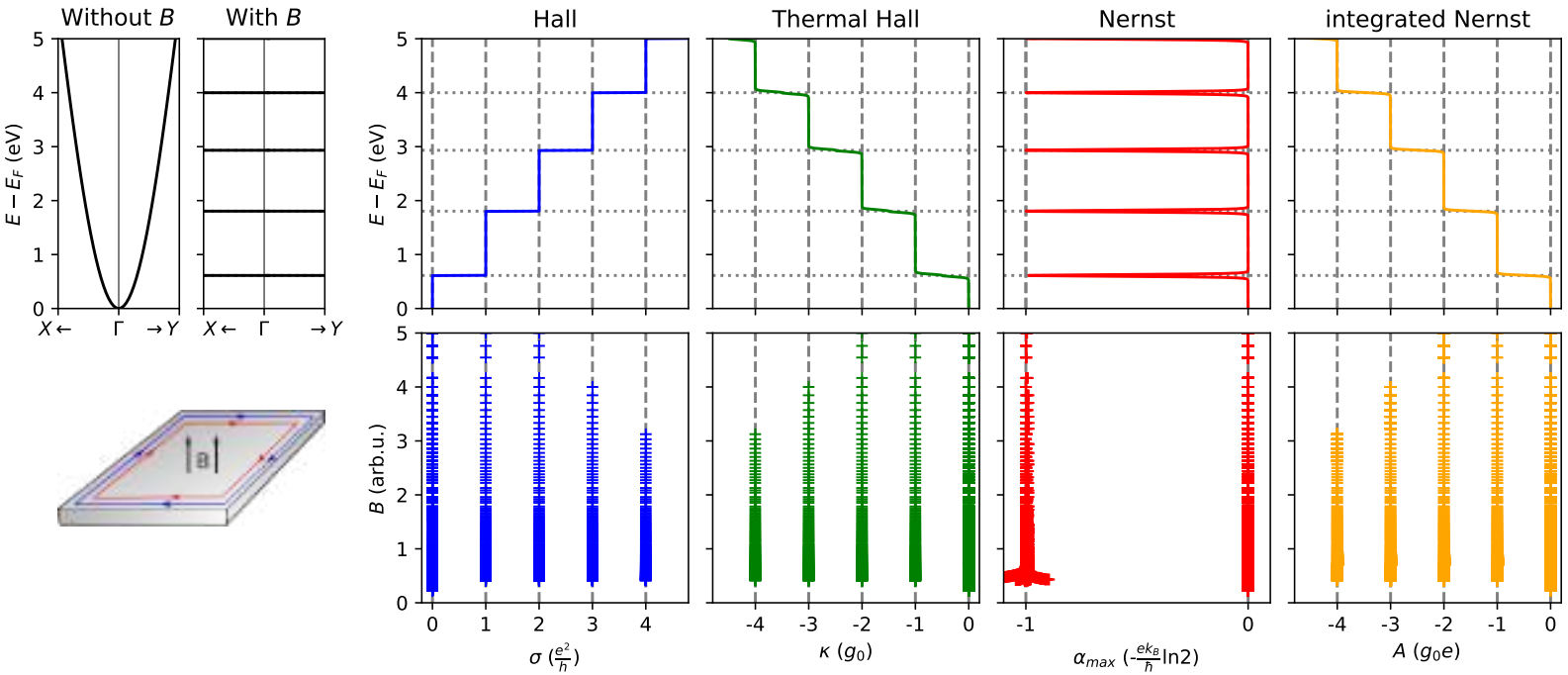

[11] JN *et al.*, submitted to Semiconductor Science and Technology (2020)

Anomalous transport in topological metals

3D free electron gas with external magnetic field

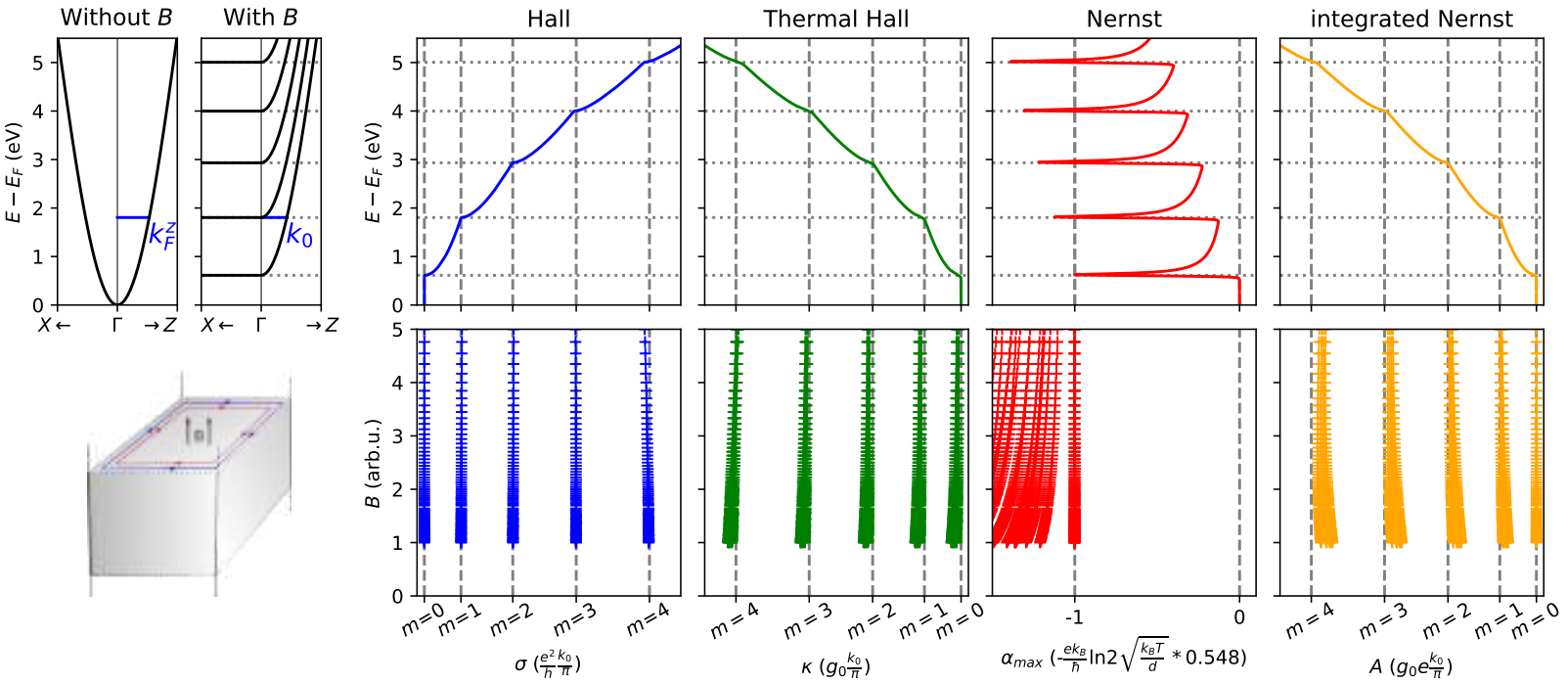

[11] JN *et al.*, submitted to Semiconductor Science and Technology (2020)

Anomalous transport in topological metals

2D Haldane model

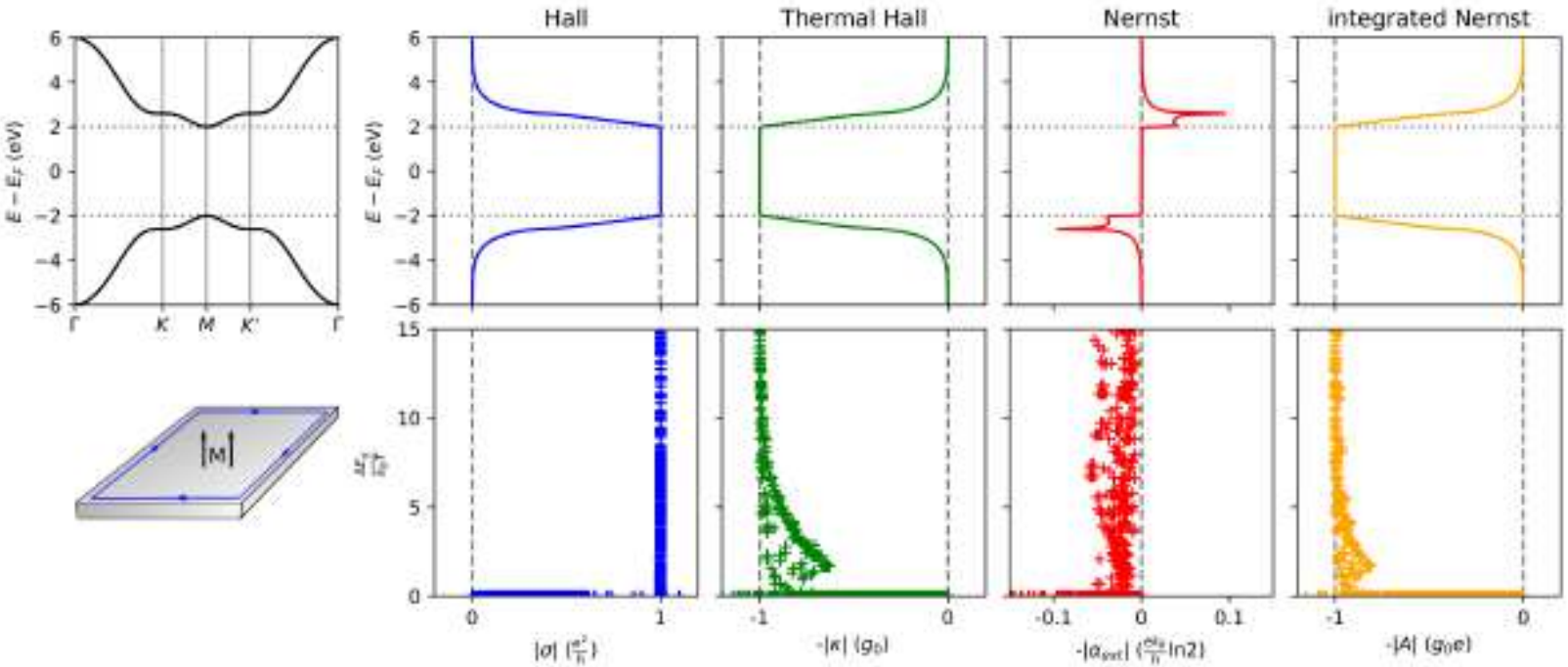

[11] JN *et al.*, submitted to Semiconductor Science and Technology (2020)

Anomalous transport in topological metals

3D expansion of the Haldane model

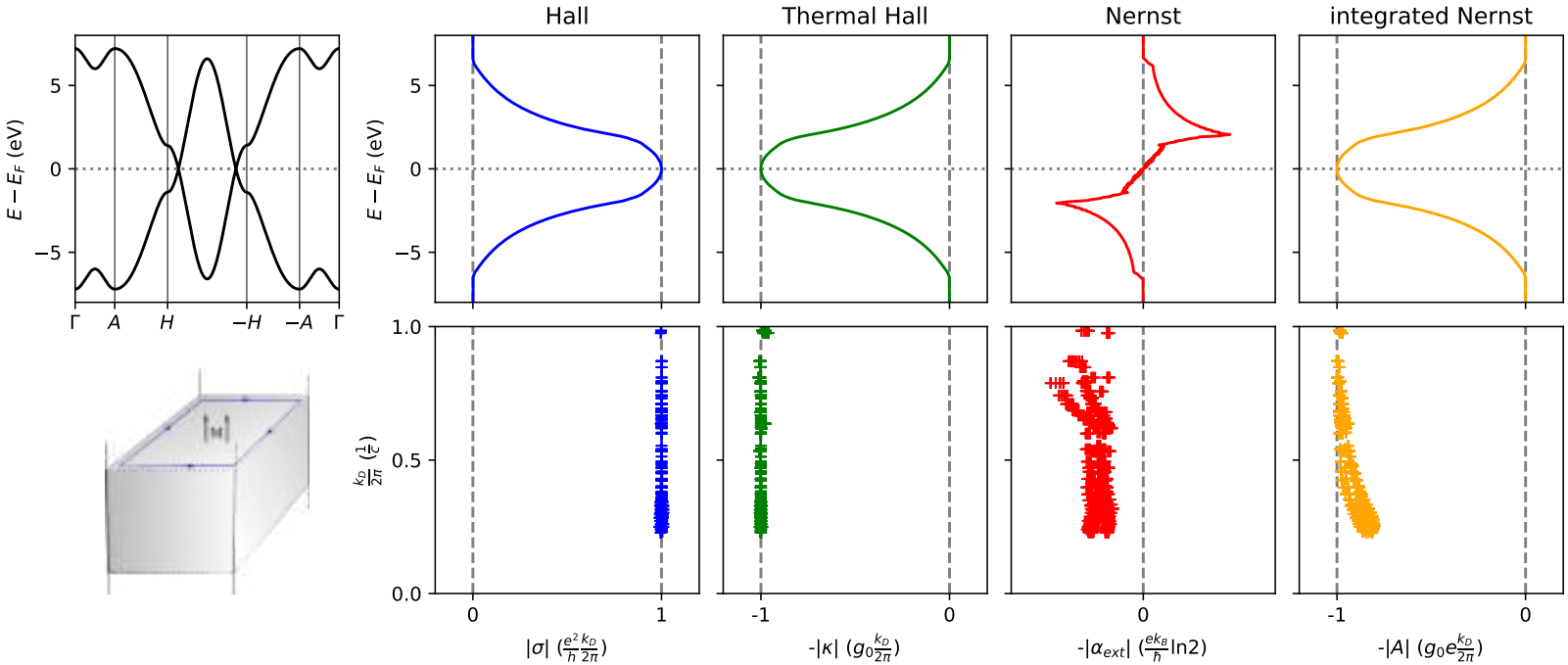

[11] JN *et al.*, submitted to Semiconductor Science and Technology (2020)

Anomalous transport in topological metals

Tabular results for the quanta

	σ	κ	α^{ext}	A
2D free	$\frac{e^2}{h}$	$-g_0$	$-\frac{ek_B}{h}\ln 2$	$-g_0 e$
3D free	$\frac{e^2}{h}\frac{k_0}{\pi}$	$-g_0\frac{k_0}{\pi}$	$-\frac{ek_B}{h}\ln 2\sqrt{\frac{k_B T}{d}}0.548$	$-g_0 e\frac{k_0}{\pi}$
2D Haldane	$\frac{e^2}{h}$	$-g_0$	*n.a.*	$-g_0 e$
3D Haldane	$\frac{e^2}{h}\frac{k_D}{2\pi}$	$-g_0\frac{k_D}{2\pi}$	*n.a.*	$-g_0 e\frac{k_D}{2\pi}$